Chem Soc Rev

REVIEW ARTICLE

View Article Online
View Journal | View Issue

Cite this: *Chem. Soc. Rev.*, 2020, **49**, 1977

Received 15th November 2019

DOI: 10.1039/c9cs00686a

rsc.li/chem-soc-rev

Steroidal supramolecular metallogels

Riikka Kuosmanen, Kari Rissanen * and Elina Sievänen *

The review deals with an expanding number of steroidal compounds that are capable of forming a metallogel providing a multitude of novel materials rich in their properties. The future of steroidal metallogels holds a myriad of potential applications as new intelligent materials. Detection of potentially harmful compounds without expensive instrumentation, entrapment of environmentally hazardous substances, and sensitive and selective nanomaterials represent only a few of these potential applications. This article reviews the design, synthesis, characterization, and applications of steroidal metallogels.

1 Introduction

The first steroidal supramolecular metallogel was observed in 1913.[1] Since then, a myriad of steroidal as well as other supramolecular (metallo)gels have been discovered. Although supramolecular gels have been utilized in various branches of science, supramolecular metallogels are a relatively new area in the field. It has gained increasing interest only in the 21st century.

Multiple biologically significant natural products belong to the group of steroids. Animal steroids, such as cholesterol, bile acids, corticosteroids, and mammalian sex hormones, contain a cholesterol-derived backbone. Cholesterol itself is essential for the function and structure of animal cell membranes, where it effects on the membrane fluidity, microdomain structure, and permeability. It acts as a precursor for steroid hormones, bile acids, vitamin D, and lipoproteins, but also correlates with harmful conditions, such as cardiovascular disease, atherosclerosis, and gallstones.[2] The chemical structure of plant sterols is similar to that of cholesterol, differing mainly in the side chain. Similarly to cholesterol in animal cells, the phytosterols in plants impact on the structure and function of the cell membranes by controlling their fluidity and permeability. The most common representatives of phytosterols are sitosterol, stigmasterol, and campesterol.[3]

Gels can be found everywhere in our daily life; hair gels, toothpaste, and soft contact lenses represent common examples

Department of Chemistry, University of Jyväskylä, P.O. Box 35, FI-40014, Finland. E-mail: kari.t.rissanen@jyu.fi, elina.i.sievanen@jyu.fi

Riikka Kuosmanen

Riikka Kuosmanen obtained her MSc in Organic Chemistry in 2014 at the University of Jyväskylä, Finland. She is currently doing her PhD on steroidal supramolecular metallogels under the supervision of Professor Kari Rissanen and Docent Elina Sievänen.

Kari Rissanen

Kari Rissanen got his PhD degree in chemistry at the University of Jyväskylä, Finland, in 1990. From 1993 to 1995 he was an associate professor in organic chemistry at the University of Eastern Finland (Joensuu). Since 1995 he has been the professor and head of organic chemistry laboratory and the leader of the supramolecular chemistry research group at the University of Jyväskylä, Finland. His research focuses on weak non-covalent, viz. the supramolecular, interactions occurring in recognition and self-assembly events studied with single crystal X-ray diffraction in the solid-state, NMR in solution and mass spectrometry in the gas phase.

of everyday applications of gels. Gels are generally considered to comprise of an elastic cross-linked network and the entrapped liquid. They have a solid-like rheology, although they mainly consist of liquid; typically gels contain 99% (w/v) of liquid, while the rest is the gelator. In supramolecular gels the low molecular weight gelators (LMWGs) self-assemble *via* non-covalent interactions (*e.g.*, hydrogen bonds, π–π stacking, metal coordination, electrostatic, van der Waals, or dipole–dipole interactions) to form the network that is then capable of entrapping the liquid.[4]

Depending on the nature of the liquid, gels can be divided in organogels (organic solvent) and hydrogels (water).[4] Gelator–gelator and gelator–solvent interactions play important roles in gel formation,[4a] which is why molecular level interactions need to be considered in correlating the gelator behavior with a given solvent. Prediction of gelation properties is thus challenging and comprehensive solvent screening tests are often required. In a typical gelation experiment a solution containing the gelator is heated above T_{gel} and the resulting solution allowed to slowly cool. The material is defined as a gel if upon inversion it is able to support its own weight. In some cases gelation can be brought up by ultrasound treatment or mechanical shaking.[4b]

Supramolecular gels have innumerable applications in different fields ranging from regenerative medicine and tissue-engineering to nanoelectronics.[5,6] They can, for example, be utilized as long-term releasers of cancer drugs applied locally after tumor removal,[7] as moulds for porous materials,[8] or in cation and anion recognition.[9]

Supramolecular gels comprise an intriguing and a very contemporary research field owing to the challenges in defining the structure of the molecular network and the properties of the resulting gels. Over the last few decades, NMR, SEM, XRD, and other techniques have developed tremendously, giving new ways to study gels and their properties.[4b,10] More elaborate liquid and solid state NMR techniques have enabled the study of the gelator molecules and gels in more detail in their native forms. Besides NMR spectroscopy, electron microscopy and powder X-ray diffraction may give insight into the organization of the fibrous nanostructures induced by the gelator molecules. High resolution pictures of xerogels and wet gels can be obtained with the help of SEM and cryo-SEM, respectively. By using field emission SEM (FE-SEM) ultra-clear, less electrostatically distorted images of the self-assembled nanostructures in the gels can be achieved.[11] Furthermore, powder X-ray diffraction (PXRD) of the xerogels has been used to provide information on the solid-state-like organization of the gelator molecules.[12] The rheological properties of the gels reveal, for example, how different stimuli change solid and fluid mechanics of the gels.[10] Furthermore, UV-vis and fluorescence titrations,[9b] impedance spectroscopy,[9b] and differential scanning calorimetry (DSC)[11] have been utilized in the research of supramolecular gels.

In metallogels metal ions take part in the process of self-assembly that leads to gelation. The metal ions may act as functional or simply coordinating entities,[4b,10] being part of or auxiliary to the gelator. In the latter case, metal ions (or a mixture of metal ions) are added as a solution to the gel or to a solution containing the gelator.[13a,14] The properties of metal ions, such as luminescence, open up a totally new field of applications for the gels,[13] and for example the luminescent properties of the lanthanide-containing metallogels have been widely studied.[15] Compared to traditional supramolecular gels, metallogels are able to respond to a wider range of physical and chemical stimuli. As a result, metallogels responding to multiple stimuli in intelligent materials may be part of our everyday lives in the future.

In metallogels, such as in supramolecular gels in general, self-assembly is a hierarchical process (Fig. 1). At first molecules form pairs, which then assemble into oligomers. Polymers are constructed from oligomers in the second phase. When the polymers interweave, thicker fibres are formed. These interweaved polymer fibres interact with each other *via* non-covalent interactions to give rise to the 3D networks, which are capable of immobilizing the solvent.[13] The properties of the metallogels in particular, may be controlled or regulated by two principal methods: by selecting the metal-ion or by introducing changes in the structure of the gelator.[10,13b]

Metallogels may form either by metal–ligand coordination upon addition of metal ions or by immobilization of solvent molecules by metal complexes. Depending on the way in which the metal-ions are incorporated into the gel network, the nature of the self-assembly process may vary. The metal to ligand ratio is defined by the properties of both the metal ion and the ligand. Labile metal ions tend to form complexes containing one metal-ion and several ligands. Ligands can adopt different coordination geometries, and in some cases the interactions with metal ions can be reversible. Typically in these cases the gel forming network arises from hydrogen bonds, van der Waals-forces, *etc.*

Elina Sievänen

Elina Sievänen studied Organic Chemistry at the University of Jyväskylä, Finland, where she obtained her PhD in 2003. From 2004 to 2007 she worked as an Academy of Finland Postdoctoral Researcher and from 2007 to 2014 as an Academy Research Fellow. In 2007 she was appointed as a Docent and in 2014 as a University Lecturer in Organic Chemistry at University of Jyväskylä. Her research interests focus on Supramolecular Chemistry, Bio-organic Chemistry and NMR spectroscopy.

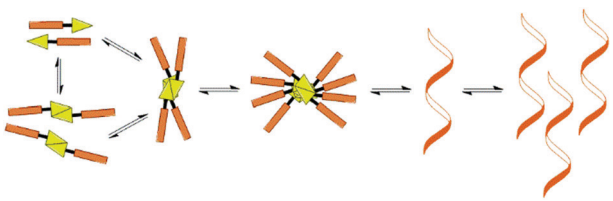

Fig. 1 Hierarchical self-assembly resulting in a supramolecular gel.[10]

Metal ions are also able to connect gelator molecules to each other, forming long chains. The formation of the 3D network in this case is based on metal coordination and is likely to be irreversible.[10,13b]

Metallogels have a tremendous amount of potential applications ranging from medicine to storage of information.[10,13a,b,14] Metallogels, as other supramolecular gels, can be utilized as moulds in preparation of various materials. Also steroid-derived metallogels have been widely used for this purpose. Ln(III)-cholate gels, for example, have been applied as moulds in nanoparticle and nanotube preparation.[11,16c,d,17] Calcium cholate hydrogels, which were utilized as moulds for palladium nanoparticle synthesis and further as reaction media, were even observed to possess remarkable catalytical properties.[18] A lanthanide-containing bile acid-based hydrogel as a template enabled the *in situ* synthesis of lanthanide trifluoride nanoparticles even at room temperature.[19] Ln(III) cholate gels have also been applied in detection of a multitude of analytes.[20] Additionally, Cu(II) lithocholate hydrogel was used as a template for the preparation of CuS nanoparticles, which were successfully used in detecting ssDNA.[16a] One of the many future applications of metallogels, steroidal ones included, may be the separation of toxic dyes from wastewaters.[21] Metallogels may also find use in electronic devices. For example, white light emitting materials, such as a cholate–lanthanide hydrogel,[22] are important in manufacturing displays.

2 Steroidal metallogels

2.1 Ferrocene derivatives

Conjugates of ferrocene and steroids were found to self-assemble into vesicles in oxidized form in the 1990s for the first time.[23] Generally ferrocene conjugates have been observed to form gels poorly because of the non-polar nature of ferrocene.[24] Ferrocene derivatives belong to the ALS-type of compounds. ALS-compounds consist of an aromatic part (A), which is connected with a (carbon) chain (L) to a steroid (S) (Fig. 2). The steroid molecule is typically cholesterol.[12,25]

Cholesteryl glycinate ferrocenylamide (Fig. 2, compound **1**) was observed to form a gel in EtOAc faster and in lower concentration than, for example, in alcohols.[12] In the SEM images of the xerogel samples of compound **1** divergent structures were detected, depending on whether the gel had been formed in EtOAc or in 1,5-pentanediol (Fig. 3). The xerogel structures obtained from

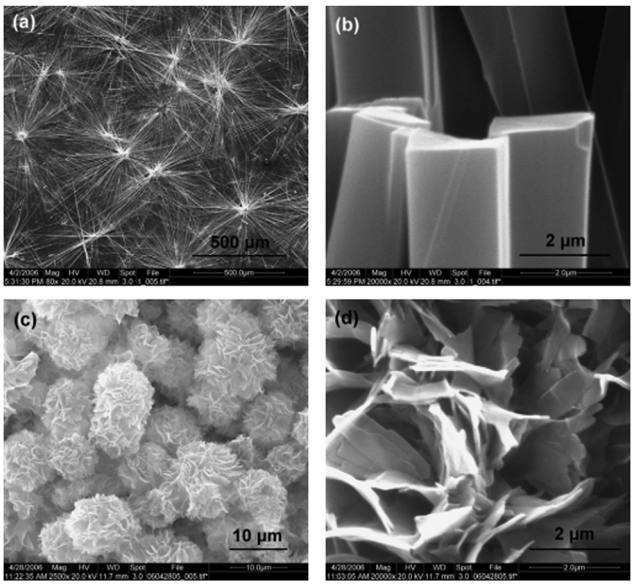

Fig. 3 SEM images of the xerogels of compound **1** obtained from ethyl acetate (a and b) and from 1,5-pentane diol (c and d). Reprinted from J. Liu *et al.*, A novel low-molecular-mass gelator with a redox active ferrocenyl group: tuning gel formation by oxidation, *J. Colloid Interface Sci.*, **318**, 397–404, Copyright 2008, with permission from Elsevier.

EtOAc resembled rod-like prisms (Fig. 3a and b), which had assembled into ball-shaped entities similar to the fluffy seeds of dandelions. The xerogel structures obtained from 1,5-pentanediol, however, possessed sheet-like structures assembled into burdock-shaped balls (Fig. 3c and d). Interestingly, in PXRD perfect lamellar structures were observed for the powder of **1** as well as for the powder of the xerogel of **1** obtained from EtOAc. Based on the XRD it was suggested that the cholesterol moieties were pointing to the sides, whereas the ferrocene moieties were stacked on top of each other.

When the alkyl chain of the diamino linker between the steroid and the ferrocene in ALS-compounds **2–5** (Fig. 4) was lengthened, the gelation ability was observed to weaken.[25a] Compound **2** with one methylene group in the chain was found to act as a supergelator, forming a gel under 1% (w/v), in cyclohexane. Compound **3** with two methylene groups formed fewer gels than **2**, and compounds **4** and **5** with three and four methylene groups, respectively, did not form gels at all. In addition to interaction between the ferrocene and cholesterol moieties, hydrogen bonding between linker chains was observed

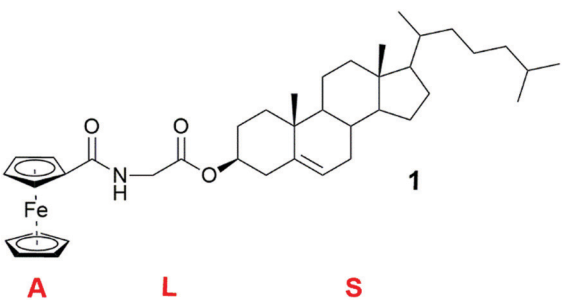

Fig. 2 Cholesteryl glycinate ferrocenyl amide (compound **1**).[12]

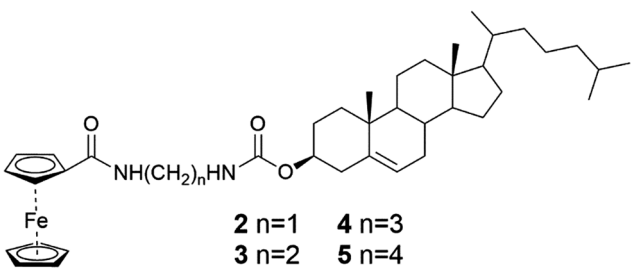

Fig. 4 Cholesterol ferrocenyl derivatives representing the ALS type.[25a]

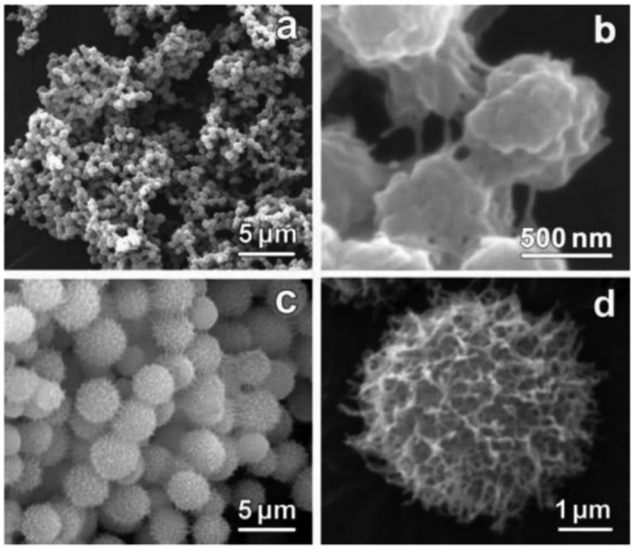

Fig. 5 SEM-images of cyclohexane xerogels of compound **2** (a and b) and compound **3** (c and d). Copyright 2008 Wiley. Used with permission from J. Liu *et al.*, An Organometallic Super-Gelator with Multiple-Stimulus Responsive Properties, *Adv. Mater.*, Wiley.

to play an important role in gelation on the grounds of FTIR- and both temperature- and concentration-depended ^{1}H NMR-measurements.

The SEM-images of the xerogels of compounds **2** and **3** (Fig. 5) showed similar ball-shaped structures than detected for the xerogels of compound **1**.[12] Compound **2** possessed different morphologies depending on the concentration: at lower concentration the gel network resembled a spider's web, whereas at higher concentration balls and fibers were observed.[25a] At the highest concentration studied only spherical objects resembling cotton balls were detected. Compared to compound **2** compound **3** formed larger ball-shaped structures, which resembled burdocks. In both cases the ball-shapes were constructed from nanofibers.

In a series of ferrocene compounds **6–8** representing the LS_2 type (Fig. 6), where two steroidal moieties are connected *via* a chain bearing the ferrocenyl part, the variations in the hydrogen-bonding capabilities were speculated to cause the different gelation properties of the compounds.[25b]

Compound **6** did not contain any hydrogen bond forming sites and did not form any gels. Compound **7** formed seven gels, mostly in alkanes. Because the gels were formed in non-hydrogen

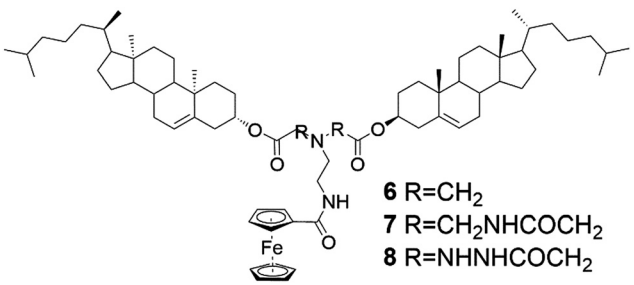

Fig. 6 Cholesterol ferrocenyl derivatives representing the LS_2 type.[25b]

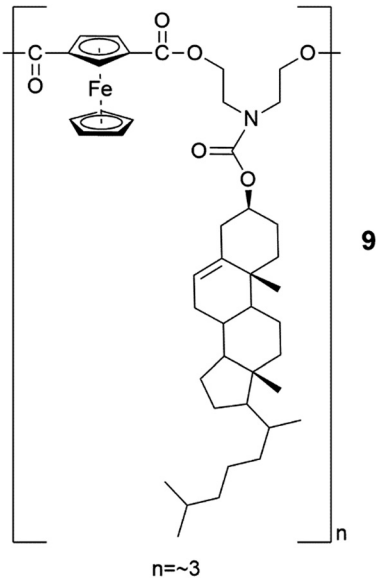

Fig. 7 An oligomer comprising of ferrocene and cholesterol (compound **9**).[25c]

bonding solvents, the formation of the gels was suggested to be based on hydrogen bonding between the gelator molecules rather than between the gelator and the solvent. This was confirmed by FTIR together with temperature- and concentration-depended ^{1}H NMR-measurements. Compound **8**, containing the largest number of hydrogen bond-forming sites within the series, formed only two gels. Too strong interactions between the molecules were speculated to hinder the gel formation.[25b]

An oligomeric compound **9** consisting in average of three cholesterols and three chains with ferrocene moieties (Fig. 7) formed a film on top of a water solution by solution casting method.[25c] The permeability studies for salts and water soluble colorants revealed that the films did not permeate red dye or copper salt (Fig. 8). Furthermore, the film was observed to support a steel ball weighing 0.88 grams, indicating better physical and chemical endurance compared to other films formed by some previously reported ferrocene-cholesterol conjugates.

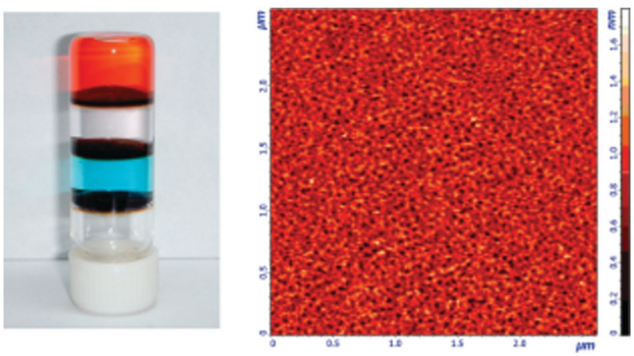

Fig. 8 Permeability test of the solution casting films formed by compound **9** (left) and AFM image of the dry, porous casting film (right). Reprinted with permission from J. Yan *et al.*, *J. Phys. Chem. B*, 2010, **114**, 13116. Copyright 2010 American Chemical Society.

2.2 Titanocene derivatives

Titanocene differs from ferrocene not only with respect of the central atom, but also on the additional two chlorines around the metal centre[26] leading to a distorted tetrahedral shape instead of the sandwich structure, which is typical for ferrocene. Titanocenes are Lewis acids, which enhances their ability to self-assemble in both polar and non-polar solvents. Titanocene derivatives containing a steroidal entity belong to the group of ALS-compounds.[24]

The titanocene moiety was found to be a prerequisite for gel formation in the series of cholesterol derivatives of titanocene (Fig. 9, compounds **10–16**).[24,27] Moreover, the length and the substituents of the carbon chain were reported to effect on gelation abilities of compounds **10–16**. The fully substituted titanocene in compound **16** was speculated to enhance the solubility of the compound to an extent capable of inhibiting gelation.[24,27] When comparing the gelation properties of compounds **10**, **12**, **14**, and **15**, however, monosubstitution on the titanocene was found to have less impact on the gelation tendency than the length or substitution of the carbon chain. Consequently, the gel forming abilities of compounds **14** and **15** bearing monosubstituted titanocene entities were similar to the gelation behaviour of compound **10** with a non-substituted titanocene moiety. The gel forming tendency of compound **12** with a non-substituted titanocene but a substituted carbon chain, on the contrary, was less effective when compared with compounds **14** and **15**. This was hypothesized to be due to the bulky cyclohexylidene groups. The lack of substituents on the carbon chain was interestingly observed to scale the gelation ability down as compound **13** did not form any gels. A longer carbon chain, on the other hand, had an adverse effect on the gel formation ability, which was obvious from the comparison between compounds **10** and **11**. The addition of one methylene group to the chain had significant effects on the gel formation, which was speculated to be due to a more flexible structure.

The impact of the substituents on the carbon chain was studied in more detail by comparing the conformations and gelation tendencies of compounds **10**, **12**, and **13**.[27] The super-gelator property of compound **10** was speculated to stem from multiple favourable conformations arising from methyl groups and hydrogens of similar size. In the case of compound **13** with an unsubstituted carbon chain, the ester group between the steroid and the carbon chain was found to point away from the titanocene part, resulting in incapability of gel formation. On the contrary, compound **12** with the geminal cyclohexylidene groups as substituents got the ester group to orient towards the titanocene moiety resulting in gel formation in both polar and non-polar solvents. Although compound **12** formed gels in higher concentrations than compound **10**, the orientation of the ester group clearly had an impact on the gel formation properties.

Gels formed by compound **10** were found to be thermo-reversible during temperature-depended ^{1}H NMR and CD measurements.[24] With both methods the self-assembly of the gel network and the structural chirality of the gel induced by the cholesterol moieties were observed. In TEM-, cryo-SEM-, and AFM-images both left- and right-handed rope-like bundles of fibres were detected. This handedness of fibres was probably due to the structure resembling spiral staircase brought about by cholesterol moieties (Fig. 10).

From the TEM- and cryo-SEM-images of the gels formed by compounds **10**, **11**, and **12** rope-like bundles of fibres were detcted.[27] Tightness of the assemblies varied from compound **10** forming the tightest and compound **11** the loosest assemblies. Moreover, compound **10** formed 3D-networks, where single fibres were connecting the rope-like assemblies together. These connecting fibres were, however, not present in the xerogels obtained from compound **12**, implicating steric hindrance in the self-assembly process due to the bulky substituents in the

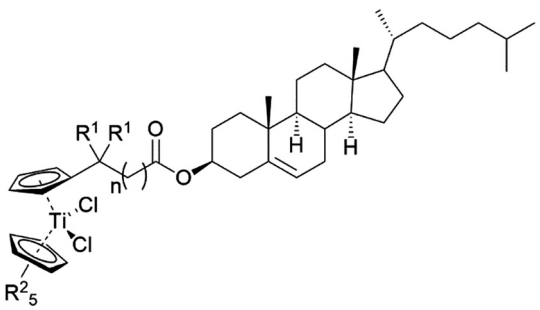

10	R^1=CH_3	$(R^2)_5$=$(H)_5$	n=1
11	R1=CH_3	$(R^2)_5$=$(H)_5$	n=2
12	R^1=$(CH_2)_5$	$(R^2)_5$=$(H)_5$	n=1
13	R^1=H	$(R^2)_5$=$(H)_5$	n=1
14	R^1=CH_3	$(R^2)_5$=$(H)_4$, CH_3	n=1
15	R^1=CH_3	$(R^2)_5$=$(H)_4$, $(C(CH_3)_3)$	n=1
16	R^1=CH_3	$(R^2)_5$=$(CH_3)_5$	n=1

Fig. 9 Cholesteryl titanocenyl derivatives **10–16**.[24,27]

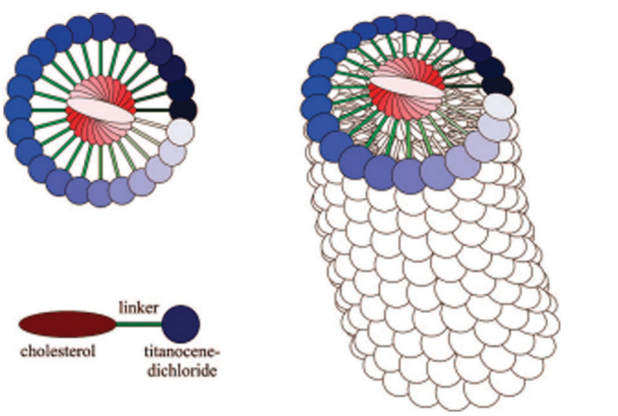

Fig. 10 Cholesterol staircase. Reprinted with permission from A. Gansäuer *et al.*, *Organometallics*, 2009, **28**, 1377. Copyright 2009 American Chemical Society.

carbon chain. In the gel formed by compound **10** both left- and right-handed assemblies were observed in the TEM- and AFM-images. Based on the CD experiments, the left-handed assemblies were observed to dominate over the right-handed ones. Temperature-depended CD revealed the self-assembly to be non-racemic and induced by van der Waals-forces between the cholesterol moieties.

2.3 Metallogels formed by bile salts

The lanthanide ions are extensively studied owing to their exceptional luminescence properties.[28] The colour of the emission is sharp and characteristic to each element in the lanthanide series. Additionally, lanthanide emissions have long lifetimes. To achieve an intense emission, the lanthanide has to form a complex with a suitable ligand. When lanthanides are combined with bile salts and a suitable solvent, the resulting materials have shown potential as emitting coating agents with chromophores,[15a,b] as templates for nanomaterials[16c,d] and nanostructures,[17,29] and as new composite materials.[30] They have even shown enzyme-induced luminescence[20b,c,31] opening up possibilities for medical applications.

The research group of Maitra[15] has studied extensively the use of lanthanide ions in bile salt-derived supramolecular gel systems. As an example, pyrene chromophore was introduced inside the sodium cholate (Fig. 11, compound **17**) micelles to which Eu(III)–salt solution was added with the aim of obtaining a more intense lanthanide emission.[15a] As a result a metallogel, in which the chromophores were in close vicinity of the lanthanide ions, was formed. The formed gels were opaque, which made comparison between the fluorescence spectra of the gels with and without the chromophore feasible. Gels with the chromophore had almost 1000% more intense luminescence compared with the gel lacking the chromophore. In addition to Eu(III), sodium cholate was found to form hydrogels with several other lanthanides including Nd(III), Sm(III), Gd(III), Tb(III), Dy(III), Ho(III), Er(III), Tm(III), and Yb(III).[15b] Rheological studies indicated a decrease in the elasticity of the gel as a function of the size of the lanthanide in question. The most elastic gel was formed with Nd(III) and the least elastic one with Yb(III).

With the aim of making the Tb(III)-cholate hydrogel sensitive to UV-light, the effect of different chromophores were studied.[15b]

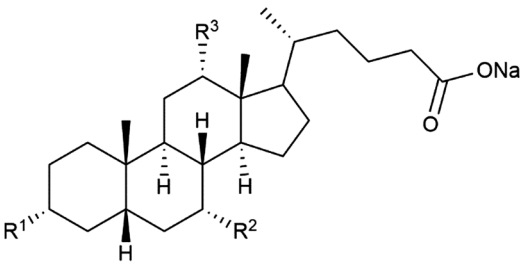

17 R^1=OH, R^2=OH, R^3=OH
18 R^1=OH, R^2=H, R^3=OH
19 R^1=OH, R^2=H, R^3=H

Fig. 11 Sodium salts of the bile acids.[37]

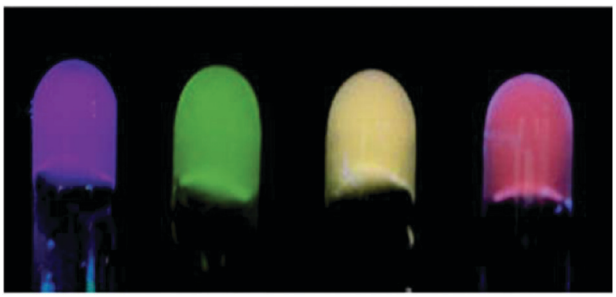

Fig. 12 Cholate hydrogels from left to right: Eu(III) cholate with pyrene; Tb(III) cholate and two Tb(III)–Eu(III) cholate mixtures all with divergent ratios of Tb(III) and Eu(III) (all with DHN). Photographs of the gels were taken under UV irradiation of 365 nm. Reproduced from S. Banerjee *et al.*, *Soft Matter*, 2011, **7**, 8207, with permission from the Royal Society of Chemistry.

Of the tested chromophores, 2,3-dihydroxy naphthalene (DHN) proved to be the best one. By preparing a series of cholate gels containing Tb(III) and Eu(III) in different ratios with DHN, divergent colours under UV-light were observed (Fig. 12). Interestingly, the emissions of the lanthanide cholate xerogels were more intense than the emissions of the native gels despite of the less efficient energy transfer from the chromophore to Yb(III) or Eu(III) in the dry gel.

Tb(III)–cholate hydrogel with DHN as a sensitizer (Fig. 13a and b) was further utilized as a scaffold for luminescence resonance energy transfer (LRET).[13c] Hybrid gels with organic dye (rhodamine B or sulforhodamine 101) as an additional

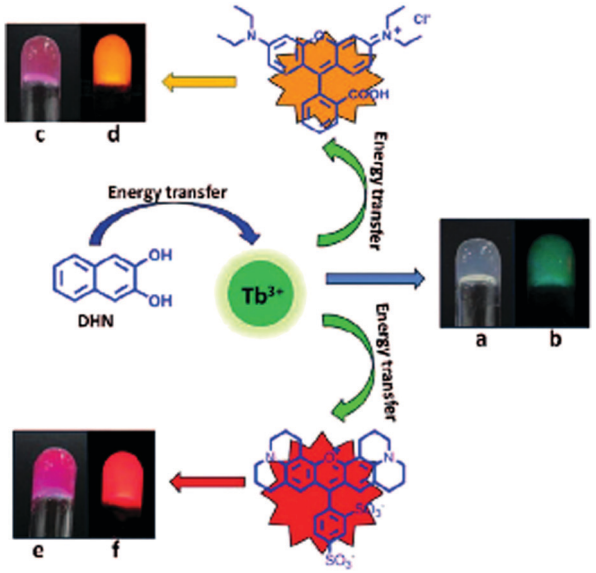

Fig. 13 Energy transfer in Tb(III)–cholate hydrogel. The gel with DHN in ambient light was colourless (a) and under UV light (365 nm) green emission (b) was observed. Cascade energy transfer with the synthetic dyes: under ambient light the gel with rhodamine B was pink (c) and the gel with Sulforhodamine 101 dark pink (e). Under UV light (365 nm) the gel with rhodamine B showed yellow emission (d) and the gel with sulforhodamine 101 red emission (f). Copyright 2017 Wiley. Used with permission from T. Gorai and U. Maitra, Luminescence Resonance Energy Transfer in a Multiple-Component, Self-Assembled Supramolecular Hydrogel, *Angew. Chem., Int. Ed.*, Wiley.

component experienced a cascade energy transfer based on time delayed excitation spectra (Fig. 13c–f). Energy transfer occurred from DHN to Tb(III) and finally to the dye. The concentration of the sensitizer (DHN) was observed to effect on the Tb(III) emissions as well as on the emissions of the dyes. With higher DHN concentration the emission intensities were increased. Xerogels were also found to be luminescent indicating that drying of the gel did not effect on the morphology of the gel. In the self-assembly model proposed, Tb(III) was speculated to act as a directing agent for gel fiber formation for the cholate molecules.[13c] The DHN molecules and the dyes then attach on the gel fibres by hydrophobic interactions. As DHN chelates Tb(III), energy transfer from Tb(III) to the dye is enabled. By confocal microscopy it was actually confirmed that the dye molecules favour attachment to the gel fiber.

The electron rich and aromatic DHN was utilized as a chromophore also in gels derived from sodium deoxycholate (Fig. 11, compound **18**) and Tb(III).[15c] A series of five different electron deficient aromatic nitro compounds was added to the Tb(III)-deoxycholate gel in a molar ratio of 1 : 1. Interestingly, 2,4,7-trinitrofluorenone (TNF) caused the emission to decrease by 63%. This phenomenon may have use in mining industry for detection of nitro compounds.

In a recent study by Laishram and Maitra[15d] the role of DHN in Eu(III)-cholate gels in different solvents was investigated. Due to quenching of Eu(III) luminescence by water it was expected that the Eu(III) luminescence, sensitized by DHN, in a Eu(III)-cholate hydrogel would be weaker than in a Eu(III)-cholate gel formed in methanol. Surprisingly, no Eu(III) emission was detected in the organogel under UV light. Based on extensive spectrometric and quantum yield measurements, it was concluded that in the case of the methanol gel the DHN is primarily in the bulk solvent. Consequently, the DHN molecules and the Eu(III) ions are too far for the energy transfer. In the hydrogel, on the contrary, the DHN molecules are in hydrophobic pockets formed by the gel fibres, which allows energy transfer and thus the Eu(III) emission can be observed.

Qiao and coworkers[32] have been active in the field of lanthanide-containing bile salt-derived supramolecular gels as well. In their study involving Eu(III)-cholate hydrogels,[32] the Eu(III)-ions were embedded inside nanofibers formed by cholate molecules. Because the Eu(III) ions were protected against the luminescence quenching by water, enhanced Eu(III) emission was observed. When the cholate concentration was increased, the emission and mechanical stability of the gel were enhanced until a point, where excess of the cholate resulted in a breakdown of the hydrogel, was reached. On the other hand, two divergent emissions were detected at low cholate concentrations, suggesting that there are two distinct environments for the Eu(III). The Eu(III)-cholate hydrogels were utilized in the preparation of Eu_2O_2S and Eu(III) doped Gd_2O_2S and Y_2O_2S nanotubes.

Sodium cholate (Fig. 11, compound **17**) and lanthanum chloride formed a gel in water at concentrations of as low as 0.04 wt%.[11] Based on DSC and rheology, heating of the gels promoted gelation and enhanced the stiffness of the gels. In TEM, SEM, and FESEM measurements temperature-depended

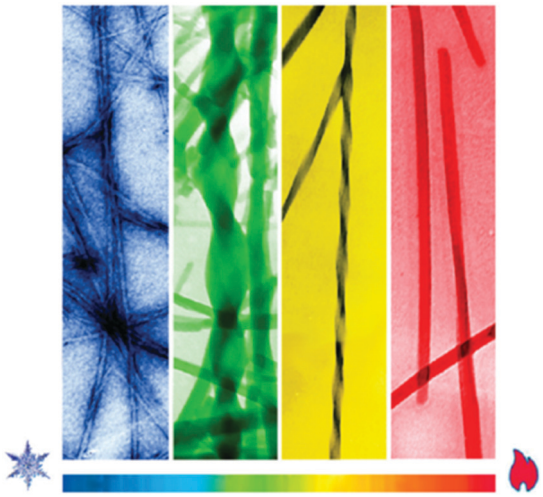

Fig. 14 Effect of temperature to the fibres of the gel formed by sodium cholate and lanthanum chloride in water. Reprinted with permission from Y. Qiao *et al.*, *J. Phys. Chem. B*, 2010, **114**, 11725. Copyright 2010 American Chemical Society.

morphology changes were observed (Fig. 14). At 4 °C hollow nanotubes were detected, but when the sample was incubated at 15 °C the number of nanotubes decreased and right-handed nanohelices started to prevail. Intertwined nanoribbons and right-handed coiled-coil rope- and pseudorope-like structures were also observed at 15 °C. At room temperature right-handed twisted and untwisted nanoribbons were present, whereas at 50 °C untwisted nanoribbons prevailed. The size of the structures increased as a function of the temperature.

Wang *et al.* have contributed to the study of lanthanide-based bile salt-derived metallogels by investigating the microstructures, rheological properties, and fluorescence of hydrogels formed with different ratios of sodium deoxycholate (Fig. 11, compound **18**) and $Eu(NO_3)_3$.[33] With equimolar amounts of **18** and Eu(III) the system self-assembled into homogeneous hydrogel at room temperature exhibiting a red-light emission under UV irradiation. With continuous addition of the europium salt a transition from a gel to a two-phase system took place. The intensity of the photoluminescence of the hydrogel was observed to strongly depend on the sodium deoxycholate : Eu(III) ratio having the maximum emission at the molar ratio of 3 : 1. Based on FTIR it was deduced that the lanthanide-deoxycholate coordination was bidentate in nature.

Bile salts have reported to form gels with other metal ions as well. For example sodium cholate formed gels in water with a series of metal ions (Fig. 15).[17] Except of Ca(II)-cholate, which required gentle heating, the gels were formed at room temperature. pH was observed to play a crucial role in the gelation process. Upon addition of the Lewis acidic metal ions, cholate anions were formed from the sodium cholate. This affected on the hydrogen bonding environment of the molecules leading either to aggregation or gelation.

The morphologies of the gels were different depending on the metal. Cd(II)- and Zn(II)-containing gels possessed tubular and entangled fibres (Fig. 16a and b) whereas the Co(II)-containing gel

Fig. 15 Metal-cholate metallogels formed in water. Reproduced from A. Chakrabarty *et al.*, *J. Mater. Chem.*, 2012, **22**, 18268, with permission from the Royal Society of Chemistry.

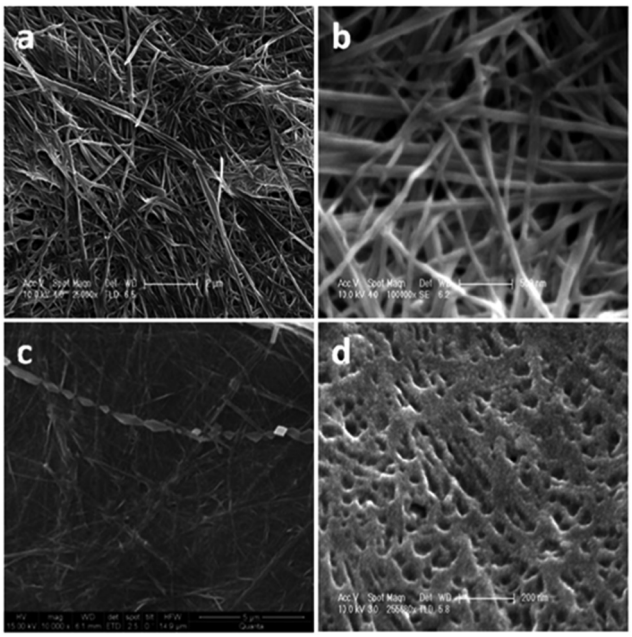

Fig. 16 SEM-images of metal-cholate hydrogels: (a) Cd(II), (b) Zn(II), (c) Co(II), and (d) Cu(II). Reproduced from A. Chakrabarty *et al.*, *J. Mater. Chem.*, 2012, **22**, 18268, with permission from the Royal Society of Chemistry.

consisted of intertwined fibres experiencing some twisting (Fig. 16c). Very thin fibers forming a porous mesh was observed in the case of the Cu(II)-containing gel (Fig. 16d). Ca(II)-cholate gel exhibited different morphologies with regard of the counter anion. The chloride salt induced formation of predominantly flat tubes, whereas with the nitrate salt nanohelices were observed. The divergent morphologies were speculated to stem from the delicate variations in the pH related to the counter anion.

Dynamic rheology measurements for the Co(II)-cholate hydrogel (Fig. 17) revealed that the gel is mechanically very stable. This was obvious from the linear domain of deformation in the frequency sweep test combined with the high yield stress value in the stress sweep test. In both of the tests the G' (elasticity) was larger than G'' (stiffness), indicating that the Co(II)-cholate hydrogel is a viscoelastic soft solid material.

Transparent Ag(I)-cholate gel consisted of spherical aggregates of various sizes, which formed a network bonding loosely to each other.[34] The gel was thermoreversible and experienced shear thinning. In addition, the gel formed again after shaking or applying pressure without any loss of mechanical strength.

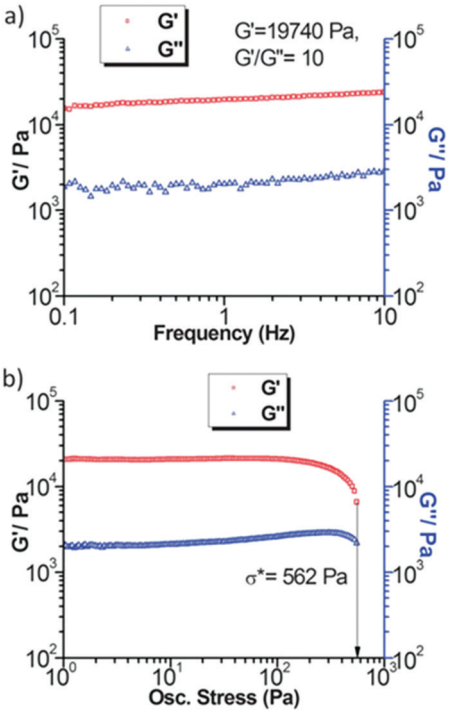

Fig. 17 Dynamic rheological measurements of Co(II) cholate hydrogel. Frequency sweep test (a) at a 1.0 Pa constant stress, and stress sweep (b) at a 1.0 Hz constant frequency. Reproduced from A. Chakrabarty *et al.*, *J. Mater. Chem.*, 2012, **22**, 18268, with permission from the Royal Society of Chemistry.

Based on the fluorescence lifetime measurements with pyrene, prodan (6-propionyl-2-dimethylamino naphthalene), and DPH (1,6-diphenylhexatriene) the cholate molecules were deduced to be compactly packed. Moreover, the gel was detected to contain areas with high hydrophobicity. The Ag(I)-cholate gel with prodan exhibited divergent colours at different temperatures (Fig. 18). Such colour changes were not observed, when a Na(I)-cholate gel containing prodan was heated.

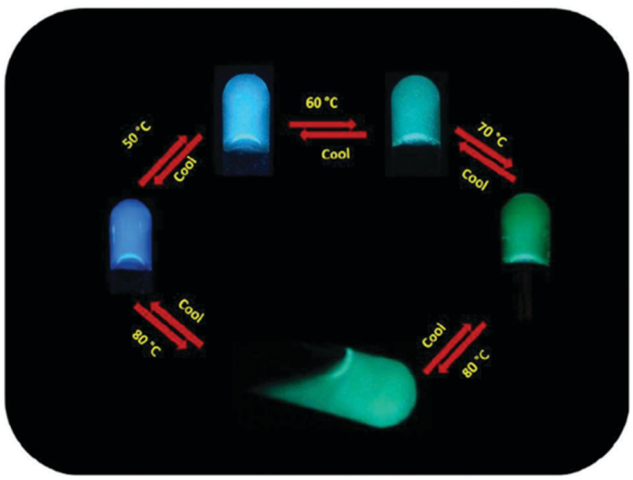

Fig. 18 Divergent colours of Ag(I)-cholate hydrogel with prodan. Copyright 2017 Wiley. Used with permission from R. Laishram and U. Maitra, A Stimuli-Responsive Metallohydrogel Exhibiting Cyclohexane-Like Hydrophobicity, Self-Assembled Supramolecular Hydrogel, *Chem. – Asian J.*, Wiley.

Indium(III) cholate and deoxycholate formed gels only after sonication of the samples.[29a] The formation of the deoxycholate gels was much slower than the formation of the cholate gels. Gelation was not observed with Al(III) and Ga(III). Elemental analysis, ESI-MS, and FT-IR measurements indicated that the gels consisted of In(III) and cholate/deoxycholate in a 1 : 3 ratio, where the cholate chelates In(III) in bidentate fashion. When the In(III)-cholate/deoxycholate gels were studies by SEM and AFM both before and after the gel formation, divergent structures were observed. In samples taken immediately after sonication but before the formation of the gel, spherical aggregates were detected. On the contrary, in the samples taken 1 h after sonication, which induced the gel formation, entangled fibres were seen. The gelation was suggested to begin by the formation of the 1 : 3 In(III) : cholate complexes. After that the complexes were speculated to self-assemble *via* hydrogen bonding and hydrophobic interactions between the cholate moieties into larger aggregates, which further self-assemble into a nanofibrous network responsible for the gel formation.

Lithocholate (Fig. 11, compound **19**) was found to form hydrogels with alkali cations (Li(I), Na(I), K(I), Rb(I), and Cs(I)).[16b] Similar to the La(III)-cholate hydrogels reported previously, the mechanical strength and the size of the structural elements increased as a function of the temperature also in the case of these alkali metal-lithocholate hydrogels.[32] Furthermore, the size of the cation affected on the stability and the transparency of the gel. The gel formed with Li(I) was the most stable and opaque, whereas the gel formed with Cs(I) was the weakest and more transparent.[16b] The different appearances of the gels was observed to stem from divergent morphologies detected by TEM and cryo-TEM measurements. Gels with Li(I) possessed nanotubules with divergent sizes, whereas the nanotubules in the cases of gels with Na(I), K(I), and Cs(I) were consistent in sizes. The increased mechanical strength observed with the increasing temperature was accompanied with a change in the appearance of the gel from transparent to opaque. Rb(I)-lithocholate gels required the highest temperatures to change, whereas Cs(I) gels disassembled when the temperature was increased. These alkali metal-lithocholate hydrogels were able to absorb virtually completely positively charged dyes (methylene blue and rhodamine 6G) in 20 minutes (Fig. 19). This phenomenon can be potentially utilized in the wastewater purification.

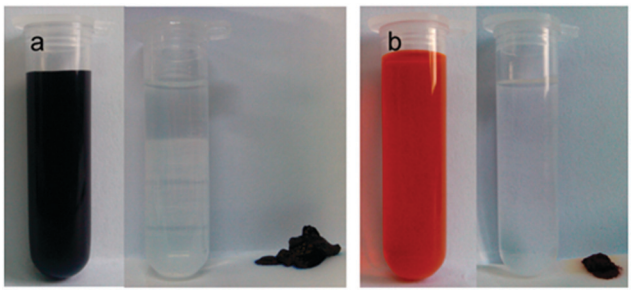

Fig. 19 Absorption of positively charged dyes by alkali metal-lithocholate hydrogels. Reprinted with permission from H. Wang *et al., J. Phys. Chem. B*, 2014, **118**, 4693. Copyright 2014 American Chemical Society.

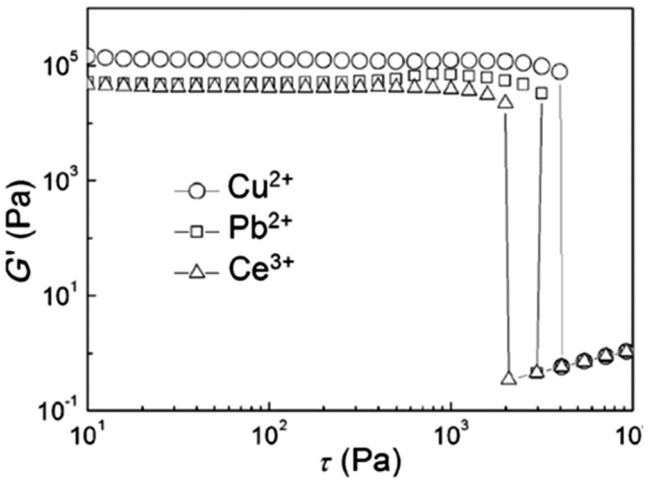

Fig. 20 Rheological measurements of hydrogels formed by lithocholate (10 mmol) and metal ions (Cu(II), Pb(II), and Ce(II) as 5 mmol at 25 °C). Storagemodulus G' is presented with respect to oscillatory stress τ. Reprinted with permission from H. Wang *et al., Chem. – Eur. J.*, 2015, **21**, 12194. Copyright 2015 American Chemical Society.

Divalent and trivalent metal ions were observed to induce metallogel formation of sodium lithocholate (Fig. 11, compound **19**) in water.[16a] It was shown that gels formed with different metal ions experienced similar mechanical stabilities (Fig. 20). The Cu(II)-lithocholate hydrogels were selected to further studies. TEM revealed that the gel consisted of a 3D fiber network showing remarkable mechanical stability that was hardly influenced by the metal ion concentration. Furthermore, the gels were thermally stable retaining mechanical strength even when heated to 90 °C. The Cu(II) hydrogel also experienced pH responsiveness. The viscosity of the solution increased as the pH was decreased from alkaline to neutral, where a gel was finally formed. Based on the FTIR spectra, the dominant interaction in the Cu(II) hydrogel was the intermolecular hydrogen bonding between the cholate molecules combined with a unidentate coordination to Cu(II) ions.

Cationic and neutral bile acid derivatives formed gels in water as well as in aqueous metal salt solutions of NaCl, $NaNO_3$, KCl, LiCl, and $BaCl_2$, for example.[35] For some derivatives gel formation required the presence of the metal. In the case of cationic derivatives the deoxycholic acid-derived ones were the best gelators. This is surprising, since deoxycholic acid derivatives do not have the tendency to form gels, as numerous studies have shown before.[36]

Metallogel formation of different bile salts (Fig. 11 and 21) with various metal ions in water with 2 : 1 or 1 : 1 (bile acid salt : metal ion) molar ratios was observed by Shen *et al.*[37] Sodium taurocholate (compound **22**) did not form any gels with the tested metal ions, whereas other bile acid salts assembled into gels with all, or some of, the metal ions tested. Sodium lithocholate (compound **19**), for example, formed gels with all the metal ions tested (Fig. 22), whereas sodium glycocholate (compound **21**) only formed five metallogels. The hydrogels formed with Ag(I) and Au(III) formed at specific pH-ranges depending on the bile salt that was used. Based on rheology (Fig. 23), the mechanical

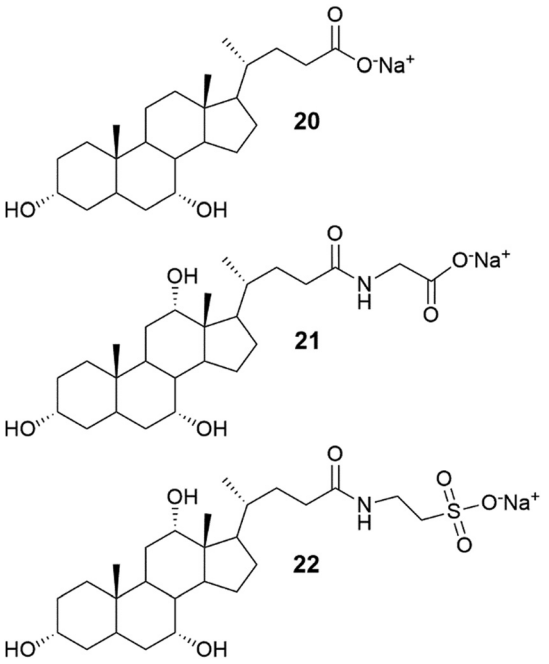

Fig. 21 Structures of sodium chenodeoxycholate (**20**), sodium glycocholate (**21**), and sodium taurocholate (**22**).[37]

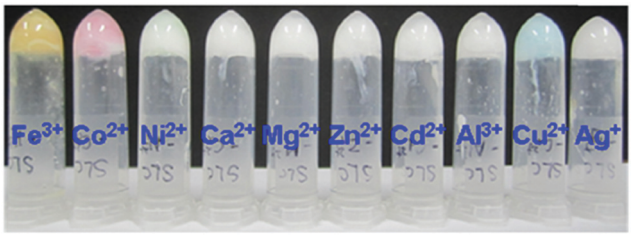

Fig. 22 Hydrogels formed by compound **19** with various metal salts. Reproduced from J.-S. Shen *et al.*, *Soft Matter*, 2013, **9**, 2017, with permission from the Royal Society of Chemistry.

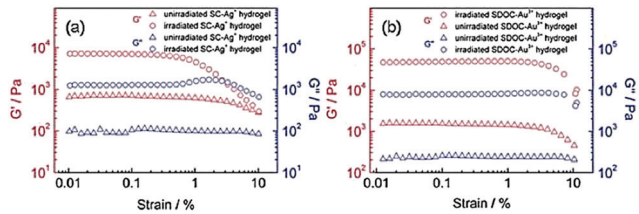

Fig. 23 Rheology measurements of the Ag(I) hydrogel formed by compound **17** (a) and Au(III) hydrogel formed by compound **18** (b). Circular and triangular symbols represent the non-irradiated and irradiated hydrogels, respectively. Storage (G') and loss (G'') moduli are plotted with respect of strain. Reproduced from J.-S. Shen *et al.*, *Soft Matter*, 2013, **9**, 2017, with permission from the Royal Society of Chemistry.

strength of the Ag(I) and Au(III) hydrogels of compounds **17** and **18** increased when the gels were irradiated with natural light in controllable light incubator (800 lux at 23 °C). This was speculated to stem from the formation of Ag- and Au-nanoparticles by photoreduction. The particles could then promote linking of the gel fibres together. However, based on the FESEM images, the irradiated and non-irradiated gels had similar morphologies consisting of 3D networks of cross-linked fibres.

Bile salt-derived metallogels have also been used in generating hybrid materials exhibiting beneficial properties. Examples include the use of Ca-doped Cd-cholate hydrogel in the presence of Na_2SeSO_3 as a template for synthesizing yellow-emitting CdSe quantum dots at room temperature[30b] and enhancement of the emission and stability of blue emitting nano clusters by incorporating them into a zinc-cholate hydrogel.[38]

The hybrid materials involving steroidal metallogels may find great potential in designing optoelectronic devices, in photocatalysis, or in biomedical and sensor applications.

2.4 Heteroatom-containing systems as coordination environments

Nitrogen and sulphur heterocycles and crown ethers are intriguing molecules regarding self-assembly with metal ions, because of their ability to form hydrogen bonds.[10,13a,b,14] Coordination to metal ions may change the properties of the heterocycle (or crown ether) leading to possibilities of developing new applications in the fields of molecular recognition, medicine, and catalysis.

Two steroid derivatives with attached nitrogen heterocycles capable of binding platinum (Fig. 24) were found to slowly form gels in various solvents.[39] Gels that were formed in solvent mixtures were more stable than gels that were formed in a single solvent. Compound **23** was observed to induce gelation in fewer occasions, but gels were more thermostable than gels formed by compound **24**. SEM-images of xerogels revealed divergent morphologies of the gel structures between the two compounds as well as between gels formed in different solvents (Fig. 25). In PhCN and DMA compound **24** formed long, thin fibres assembling into a dense network providing evidence for the better gel forming ability of the compound. Gels formed by compound **23** in the same solvents consisted of wide, ribbon-like fibres. Addition of EtOH or MeOH to DCE or chloroform affected on the morphology of the gels formed by compound **24** producing short, thick, and twisted fibres. Addition of hexane or acetone to DCE, on the other hand, revealed the gel fibres to resemble long and thin wool fibres.

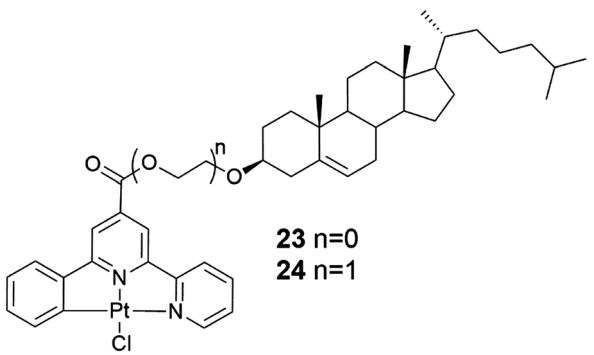

Fig. 24 Two steroid derivatives with attached nitrogen heterocycles capable of binding platinum.[39]

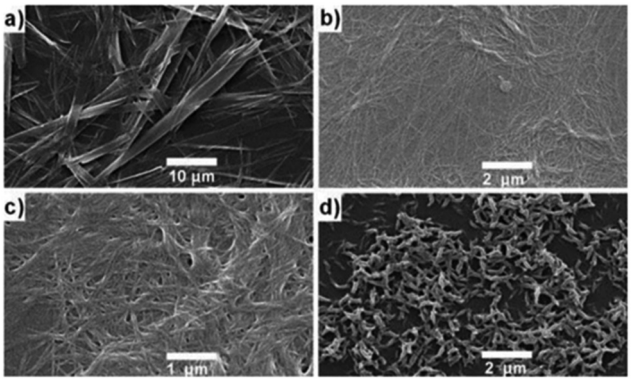

Fig. 25 SEM images of the xerogels of compounds **23** and **24**. Compound **23** in PhCN (a) and compound **24** in PhCN (b), in DCE (c), and in solvent mixture containing DCE and EtOH (d). Copyright 2011 Wiley. Used with permission from T. Tu *et al.*, Visual chiral recognition through enantio-selective metallogel collapsing: synthesis, characterization, and application of platinum-steroid low-molecular-mass gelators, *Angew. Chem., Int. Ed.*, Wiley.

The chiral recognition abilities of the gels were also studied.[39] Addition of (*S*)- or (*R*)-BINAP with heating to the 1% metallogel (compound **23** in chloroform and compound **24** in toluene) resulted in the collapse of the gel structure. This was suggested to originate from the bulky BINAP replacing the chlorine coordinated to platinum resulting in the inability of the heteroaromatic moieties to interact with one another. The gel network formed by compound **23** in chloroform collapsed after adding only 0.1 equivalents of (*R*)-BINAP to the chloroform gel making it more sensitive in chiral recognition compared to compound **24**. The addition of (*R*)-BINAP to the gel gave rise to larger, denser, and longer crystalline rods compared to the addition of (*S*)-BINAP, respectively. Addition of other phosphine ligands similarly caused collapse of the gel.

The cholesterol derivative of platinum bipyridine (Fig. 26, compound **25**) self-assembled into gels at room temperature in aliphatic solvents, such as octane.[40] It formed an exceptionally strong gel in dodecane, which was stable even after heating up to 117 °C, a temperature near the decomposition temperature of the platinum complex. SEM images showed a 3D-network

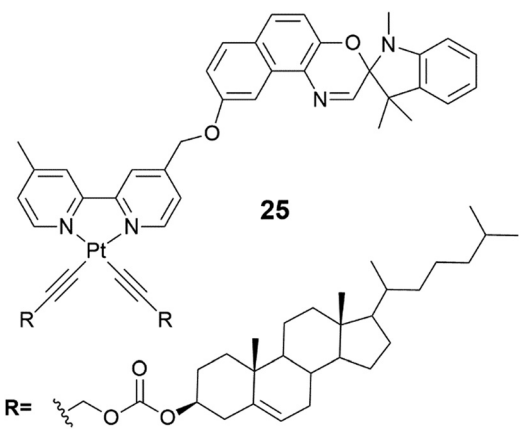

Fig. 26 Compound **25**.[40]

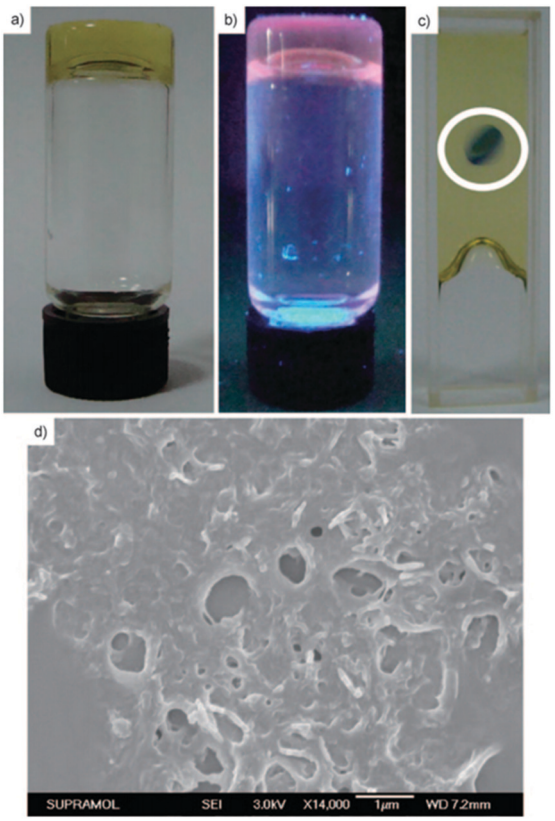

Fig. 27 Dodecane gel of compound **25** in the sun light (a), in UV-light (b), and colour change of the gel after a prolonged exposure to UV-light at 15 °C (c). SEM-image of the dried dodecane gel of compound **25** (d). Copyright 2011 Wiley. Used with permission from Y. Li *et al.*, Synthesis, Characterization, and the Photochromic, Luminescence, Metallogelation and Liquid-Crystalline Properties of Multifunctional Platinum(II) Bipyridine Complexes, *Chem. – Eur. J.*, Wiley.

formed by cross-linked fibres (Fig. 27d). Interestingly, a prolonged exposure of the gel to UV-light at 15 °C induced a colour change from yellow to blue (Fig. 27a–c). Blue colour faded back to yellow after the exposure.

The gelation properties of cholesterol based terpyridyl platinum derivatives **26** and **27** (Fig. 28) depended on the substitution of the terpyridyl moiety.[41] Compound **27** formed two gels at high concentrations (25 mg mL^{-1}) being nearly insoluble in most organic solvents. Compound **26** with *tert*-butyl substituents, for one, was

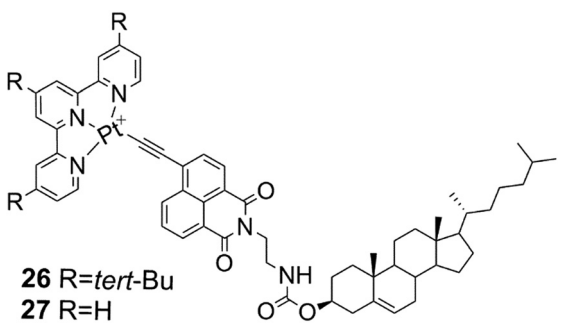

Fig. 28 Compounds **26** and **27**.[41]

soluble in most polar solvents, but formed three gels in different concentrations in toluene, ethyl acetate, and *n*-propanol. If the samples used for testing the gelation tendencies were not treated with ultrasound after heating, compound **26** precipitated out from the solution. The red precipitate formed in *n*-propanol did not experience a colour change after heating. However, the gels formed in *n*-propanol and toluene changed colour: the liquid sample was red and after the ultrasound treatment the gel changed from opaque to yellow.

The SEM- and TEM-images of the xerogel of compound **26** in *n*-propanol showed that the gel network comprised of ribbon-like, slightly twisted fibres.[41] Based on X-ray crystallography and surface wettability testing the structure of the gel was observed to form of layers. The layers were comprised of ribbon-like structures with hydrophobic cholesterol on the outside (Fig. 29, below). The precipitate, on the other hand, was detected to consist of spherical structures, which were revealed to be vesicles by TEM. The vesicle wall was found to consist of a single molecular layer with the cholesterol parts inside the vesicle (Fig. 29, above). The acetonitrile gel of **27**, for one, possessed a wrinkled surface structure covered with fibres, whereas the precipitate was observed to consist of knot-like structures with wrinkled surface.

Compounds **28** and **29** (Fig. 30) spontaneously assembled into gels during chromatography and NMR-, MS-, and IR-measurements.[42] Compound **28** acted as a supergelator, whereas compound **29** formed gels in higher concentrations (as 1%). During storage at room temperature the gels formed by compound **29** were observed to turn into solutions but were formed again after heating. When irradiated with laser beams gels of both **28** and **29** experienced Tyndall effect. Based on SEM-images the gel network comprised of compound **28** in 1 : 1 H_2O : MeOH consisted of grass-like fibres, whereas compound **29** was found to form ball-like structures both in solution and in the gel state (Fig. 31). The spherical morphology was suggested to stem from the steric hindrance of Zn-coordinated phenantroline, preventing the formation of fiber-like structures.

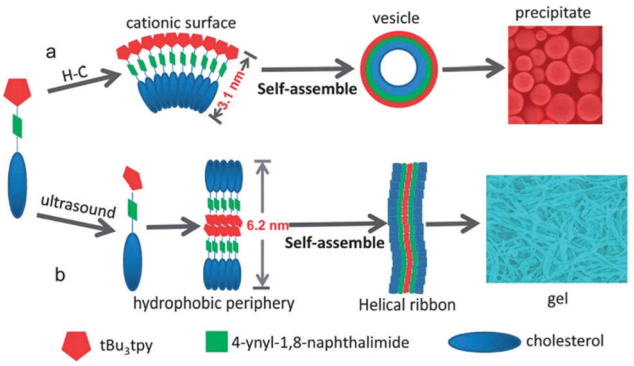

Fig. 29 Schematic representation of the self-assembly of compound **26** in *n*-propanol: above the heating–cooling cycle and below after ultrasound treatment. The pentagons represent the *tert*-pyridyl moieties, the squares naphthalene imides, and the ovals the steroid moieties. Reproduced from K. Liu *et al.*, *J. Mater. Chem. C*, 2013, **1**, 1753, with permission from the Royal Society of Chemistry.

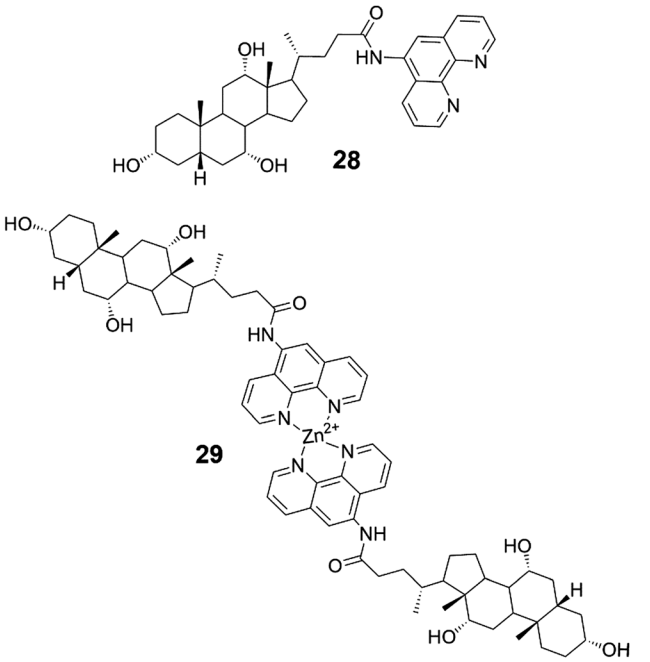

Fig. 30 The conjugate of cholic acid and phenantroline **28** and its dimeric Zn-complex **29**.[42]

From the three pyridine derivatives of cholesterol (Fig. 32) only compound **31** was observed to form a metallogel with Ag(I)OTf in diphenyl ether, despite of the better gel forming abilities of compounds **30** and **32** in pure solvents.[43] The perpendicular orientation of the pyridyl nitrogen with respect of the cholesterol moiety and the positions of the adjacent pyridyl nitrogens (appr. 180°) in the helical staircase assembly (see Fig. 10) were speculated to promote the metallogel formation.

The benzimidazole derivative of cholesterol (Fig. 33, compound **33**) was observed to form brown metallogels with silver(I) ions in 1 : 1 (v/v) DMF : H_2O.[9j] Without the silver salt **33** formed a partial gel in 1 : 1 (v/v) DMF : H_2O and no gels in other solvents or with other metal salts (Fig. 34). Based on the FTIR and ^{1}H NMR measurements combined with UV-vis and fluorescence titrations, the nitrogen on the benzimidazole moiety was responsible for the metal-coordination and also together with the ester group for the self-assembly leading to gelation. The partial gel without the silver salt had a different morphology compared to the silver gel (Fig. 35). The metallogel consisted of plate-like assemblies stacked on top of each other, whereas the partial gel contained spherical assemblies.

The silver gel of compound **33** was not thermoreversible and collapsed in the presence of Cl^- ions as AgCl formed and precipitated out from the gel network.[9j] However, the gel formed again after adding a sufficient amount of Ag(I). Interestingly, the colour of the gel was lighter than before the addition of the Cl^- ions (Fig. 36). Impedance spectroscopy in various temperatures revealed that the metallogel was able to conduct ions when thermally triggered. Rheology and impedance spectroscopy explained the ability by the presence of a disorganized rubbery state within the silver gel.

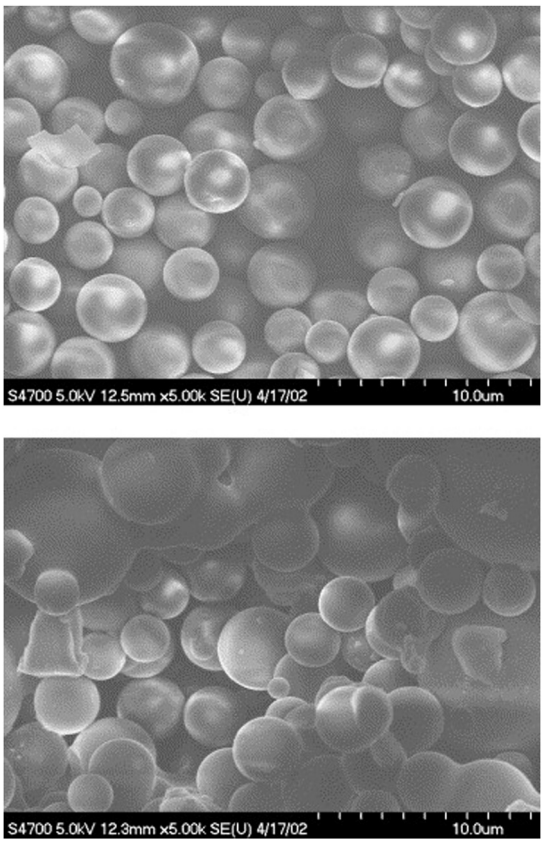

Fig. 31 SEM-images of compound **29** in 1 : 1 H_2O : MeOH. The xerogel is presented above and the solution evaporated to dryness below. Reprinted from M. Dukh *et al.*, Metal coordination as a tool for controlling the self-assembling and gelation properties of novel type cholic amide–phenanthroline gelating agent, *Tetrahedron*, **59**, 4069–4076, Copyright 2003, with permission from Elsevier.

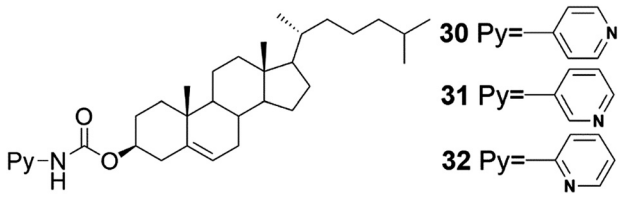

Fig. 32 Compounds **30–32**.[43]

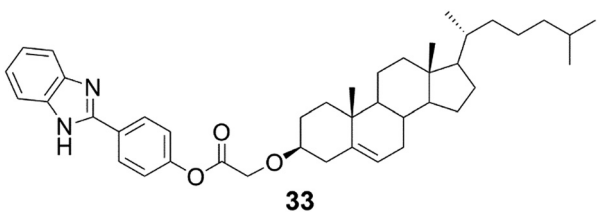

33

Fig. 33 The benzimidazole derivative of cholesterol (compound **33**).[9j]

Cholesterol appended diazine derivative (Fig. 37, compound **34**) on a 4-hydroxybenzaldehyde scaffold formed gels with Ag(I) and Fe(III) ions in $CHCl_3$: CH_3OH (3 : 1, v/v).[44] With the aid of

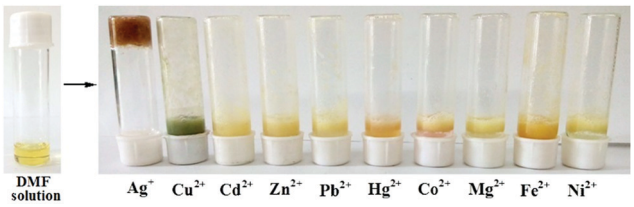

Fig. 34 Compound **33** in 1 : 1 (v/v) DMF : H_2O with different metal ions. Copyright 2017 Wiley. Used with permission from K. Ghosh *et al.*, Visual Sensing of Ag^+ Ions through Gelation of Cholesterol-Appended Benzimidazole and Associated Ion Conducting Behaviour, *ChemistrySelect*, Wiley.

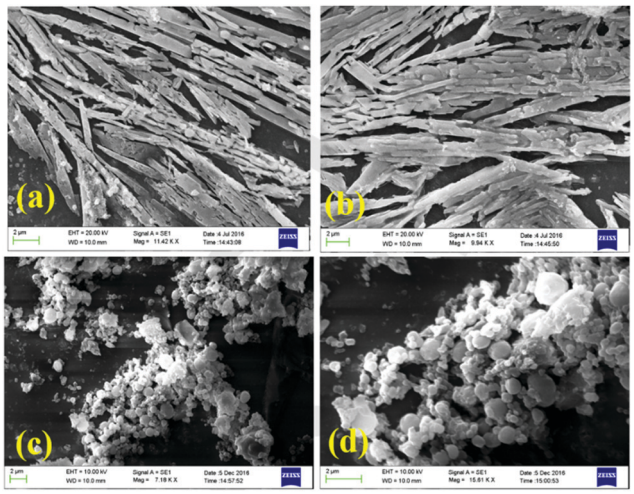

Fig. 35 SEM images of the xerogels of compound **33** in 1 : 1 (v/v) DMF : H_2O with Ag(I) (a and b), and without Ag(I) (c and d). Copyright 2017 Wiley. Used with permission from K. Ghosh *et al.*, Visual Sensing of Ag^+ Ions through Gelation of Cholesterol-Appended Benzimidazole and Associated Ion Conducting Behaviour, *ChemistrySelect*, Wiley.

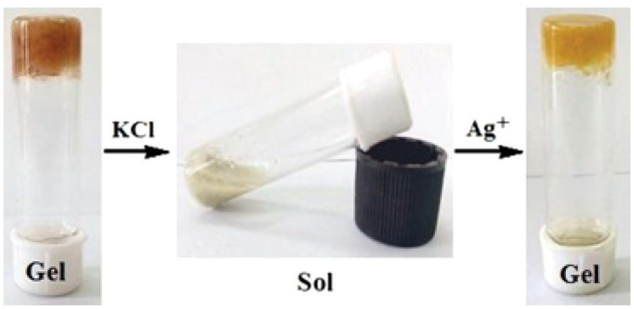

Fig. 36 Response of the silver gel (in 1 : 1 (v/v) DMF : H_2O) of compound **33** to chemical stimuli. Copyright 2017 Wiley. Used with permission from K. Ghosh *et al.*, Visual Sensing of Ag^+ Ions through Gelation of Cholesterol-Appended Benzimidazole and Associated Ion Conducting Behaviour, *ChemistrySelect*, Wiley.

FTIR and ^1H NMR the authors suggested a gelation model, where the diazine group coordinates the metal ions, which assist in the formation of the gelator network. The strong hydrophobic interactions of the cholesteryl moieties further reinforce the aggregation. When tetrabutylammoniun chloride was added to the Ag(I)-gel of **34** it broke down completely,

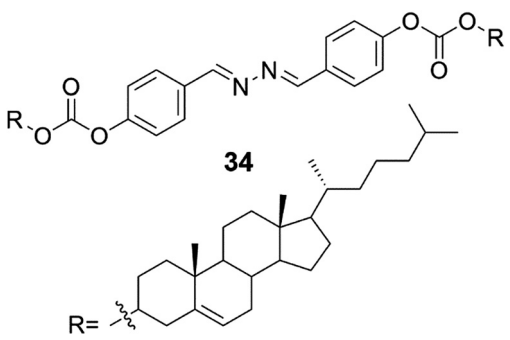

Fig. 37 The structure of compound **34** capable of forming organogels with Ag(I) and Fe(III) ions.[44]

whereas under identical conditions the Fe(III)-gel remained undisturbed. All the other halides (TBAF, TBABr, and TBAI), however, were unable to induce similar gel–sol transformation of the Ag(I)-gel. When TBAI was added into the Fe(III)-gel, a colour change from orange-red to orange, but no phase change, was observed. These properties demonstrate the usefulness of these metallogels in visual recognition and discrimination of halides. The Ag(I)-gel of **34** remained intact upon addition of NH_4SCN, whereas the Fe(III)-induced gel turned into a solution meaning that also the gels with different metal ions can be visually distinguished. It was also observed that the Fe(II) ions did not distract the Fe(III)-promoted gelation. This is very promising, since most of the Fe(III)-sensing probes suffer from interference by the Fe(II) ions. In addition to acting as materials for visual discrimination of halides or as probes for Fe(III)-sensing, the Ag(I)- and Fe(III)-metallogels of **34** were able to effectively adsorb uranine and picric acid from water being recyclable in the process.

Organogels formed by cholesterol azopyridine conjugate (Fig. 38, compound **35**) exhibited metal ion-mediated helicity inversion through metal ion coordination.[45] Compound **35** was able to form self-supporting gels after addition of Ni(II), Cu(II), Mn(II), Mg(II), Fe(II), Bi(III), and Eu(III). The gels were studied by microscopic techniques combined with FTIR, ^{1}H NMR, and CD measurements. The ^{1}H NMR experiments strongly indicated that the metal ions were coordinated with the pyridyl unit rather than with the azo moiety. When changing the metal ion from Ni(II) to Cu(II), the M-helical structure and negative CD peak were transformed into P-helical nanoribbons and positive CD signals indicating that metal ions were able to induce chirality difference in the gels. Based on CD and SEM it was established that P-type helical aggregates showed positive Cotton effects at 400–500 nm, while M-helical aggregates exhibited negative Cotton effects at the same region. The chirality of the gels depended not only on the metal ion but also on the solvent matrix. For example, the Ni(II)-gel showed M-helicity in *n*-butanol but nanostructures with P-helix were obtained in *p*-xylene : EtOH. It was observed that in solvents with relatively low polarity most of the complexes displayed P-chirality. In addition to the fascinating properties of the metallogels of **35**, the gel formed by the compound itself was prone to *E* to *Z* photoisomerization upon UV light irradiation.

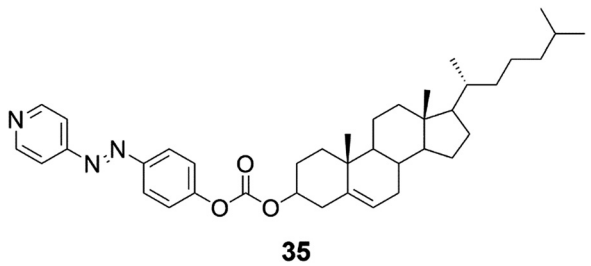

Fig. 38 The azo-cholesterol conjugate **35** capable of exhibiting photo-triggered dimensional transition and controllable supramolecular chirality.[45]

Cholesterol derivatives NiC_2 and NiC_6 containing bis(dithiolene) moiety (Fig. 39, compounds **36** and **37**) were found to form gels in linear alkanes (C_7–C_{12}).[46] The transparent, thermoreversible, and robust gels were stable for several months. NiC_2 was observed to form gels with lower concentrations than NiC_6. In dodecane NiC_2 was found to commence gelation as low a concentration as to be categorized as a supergelator. On the contrary, NiC_{11} (Fig. 39, compound **38**) and an additionally synthetized NiC_0 did not form any gels in linear alkanes, suggesting that the gel formation depended on the length of the carbon chain.

Based on SEM and AFM the gel network formed by **36** was consisted of twisted fibers, which were entangled to each other.[46] CD measurements revealed that the helicity of the gel fibers was right-handed. The helical fibers were responsible for the chiro-optical effects at the near-infrared region. The same effects, however, were not detected in the solution **36**. The formation of the gel was suggested to occur *via* hierarchical process (Fig. 40), which results in a gel network consisting of entangled twisted fibres formed from 1D helical stacks of the compound in question.

The crown ether–cholesterol conjugate **39** (Fig. 41) was found to form gels in 4 : 1 cyclohexane : benzene with divergent melting temperatures depending on the metal ion present.[47] The melting temperatures of the gels were observed to increase and then gradually decrease with respect of the increasing concentration of

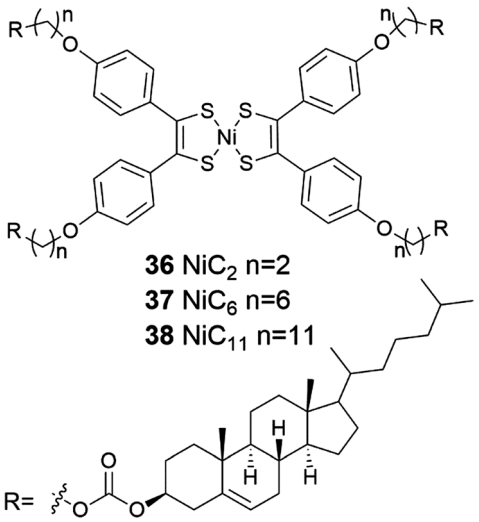

Fig. 39 Nickel-bis(dithiolene) complexes conjugated to cholesterol **36–38**.[46]

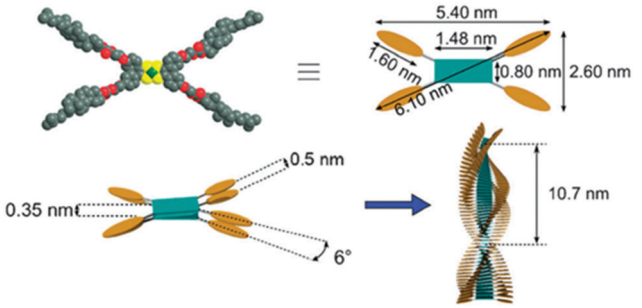

Fig. 40 A schematic representation of the hierarchical self-assembly process of compound **36** (NiC_2) in cyclohexane. Dimensions depicted were determined by AFM. Reproduced from S. Debnath *et al.*, *Chem. Commun.*, 2012, **48**, 2283 with permission from the Royal Society of Chemistry.

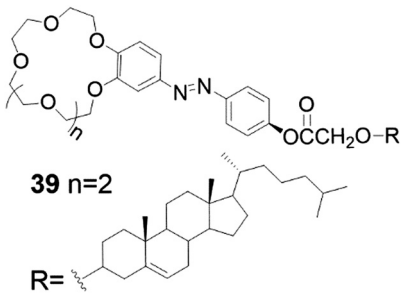

Fig. 41 Cholesterol-crown ether derivative **39**.[47]

Li(I), Na(I), K(I), Cs(I), Rb(I), and NH_4^+-salts. Particularly Rb(I) induced an increase in the melting (by 20 °C) when compared with the gel without any metal. Cs(I) had an opposite effect on the melting temperature, and above 15 mol% of Cs(I) the gelation was not even observed. This was suggested to stem from the tendency of the Cs(I)-ions to form 1 : 2 metal : crown sandwich complexes with 18-crown-6, which would then inhibit the gel formation by affecting adversely to the self-assembly process.

2.5 Gels formed by multiple components

Versatility is the asset of gels formed by multiple components.[48] Materials with very distinctive properties can be generated by mixing compounds in different ratios or by changing one or more components. Multiple component gels are commonly prepared by first synthesizing the gelators and then performing gelation tests with varying combinations and ratios of compounds in different solvents. By subcomponent self-assembly time and resources can be saved when screening potential gel forming combinations. Mixing of all the needed components forms the gelating agent *in situ*, during the gelation test.[48]

Gels formed by compounds **40** and **42** (Fig. 42) were observed to be stronger in the presence of [60]-fullerene.[49] For example, gels formed by compound **40** in benzene in the presence of [60]-fullerene were stable up to 20 °C, whereas gels without it decomposed when temperatures exceeded 5 °C. In the case of compound **42** a stable gel was formed only with [60]-fullerene at 5 °C, whereas in the absence of [60]-fullerene gelation was not observed. Compounds **41** and **43** (Fig. 42) did not form any gels

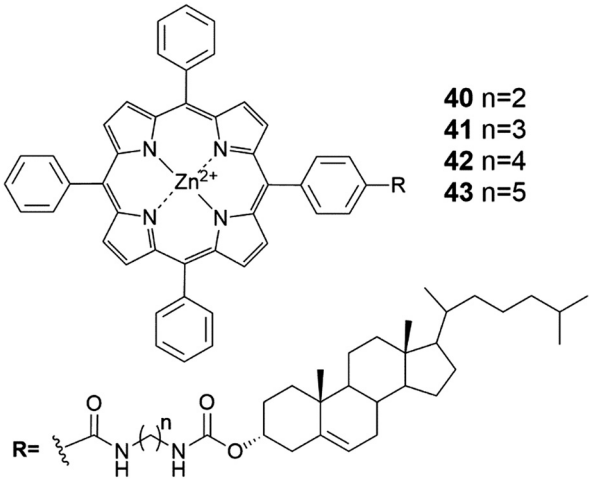

Fig. 42 The structures of cholesteryl porphyrins **40–43**.[49]

in the tested solvents with [60]-fullerene. Based on computational studies the carbon chain connecting the cholesterol and the porphyrin ring tended to bend in the case of compounds **41** and **43** having an odd number of carbons in the carbon chain. In the contrary, compounds **40** and **42** with an even number of carbons in the carbon chain possessed extended conformations. Hence, the extended conformation was more favourable regarding interactions between molecules. The cholesteryl-porphyrins formed a spiral staircase architecture suitable for accommodating the [60]-fullerene molecules between the porphyrin moieties to give rise to 2 : 1 sandwich complexes (Fig. 43), whose structures were evidenced by measuring the melting point of the gel together with

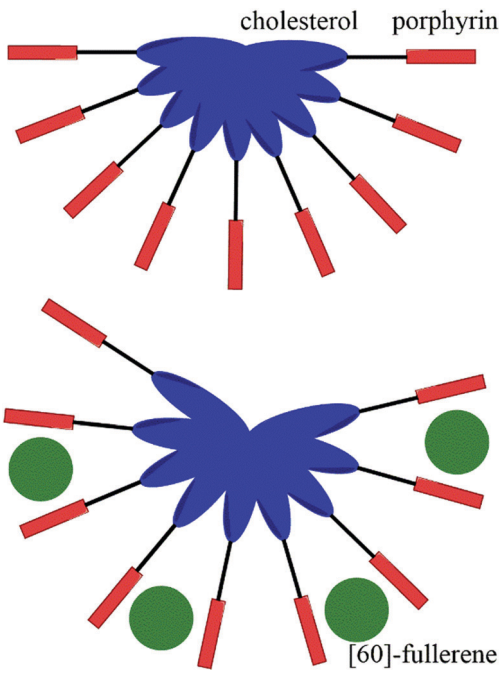

Fig. 43 The spiral staircase architecture and sandwich complexes of cholesteryl porphyrins **40** and **42**. Adapted with permission from T. Ishi-i *et al.*, *Langmuir*, **17**, 5825. Copyright 2001 American Chemical Society.

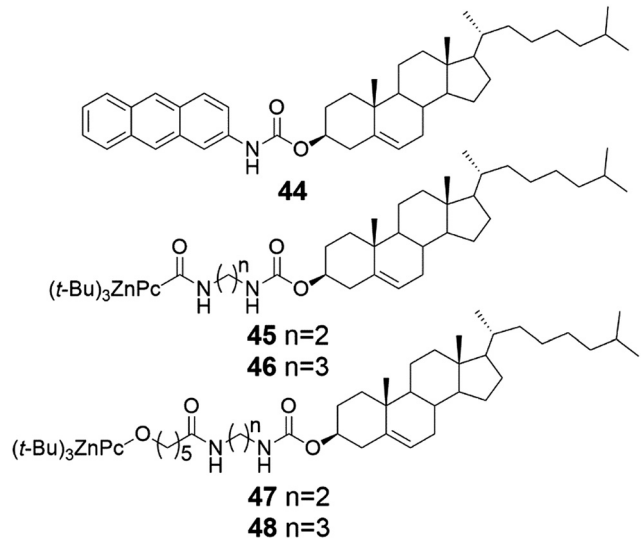

Fig. 44 Cholesteryl anthracene **44** and cholesteryl Zn^{II}-Pc-containing derivatives **45–48**.[50]

UV-vis- and CD-measurements. Based on the IR-measurements interactions between the cholesterol moieties were primarily responsible for the gel formation for compounds **40** and **42**, followed by interactions between the porphyrin moieties, and interactions between the porphyrins and [60]-fullerene.

Cholesteryl anthracene (Fig. 44, compound **44**) formed thermoreversible and photoactive gels (Fig. 45) in aromatic solvents when mixed with the ratio of 20 : 1 with Zn(II)-phthalocyanine (Zn^{II}-Pc)-containing compounds **45–48**.[50] Whether the carbon chain connecting the cholesterol and the phthalocyanine moieties possessed an odd or an even number of carbons had no effect on the mechanical stability of the gel contrary to the analogous

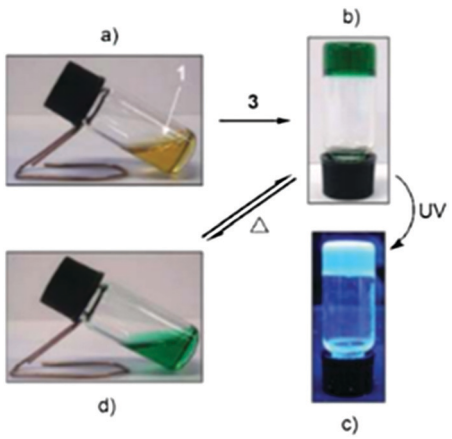

Fig. 45 Compound **44** in toluene at room temperature (a), addition of compound **45** into the solution of **44** in toluene (**44** : **45** 20 : 1) leading to gel formation after heating–cooling cycle (b), the irradiation (at 356 nm) of the photoactive gel containing compounds **44** and **45** (c), and thermoreversibility of the toluene gel of compounds **44** and **45** (d). Copyright 2008 Wiley. Used with permission from D. D. Díaz *et al.*, Strength Enhancement of Nanostructured Organogels through Inclusion of Phthalocyanine-Containing Complementary Organogelator Structures and *In Situ* Cross-Linking by Click Chemistry, *Chem. – Eur. J.*, Wiley.

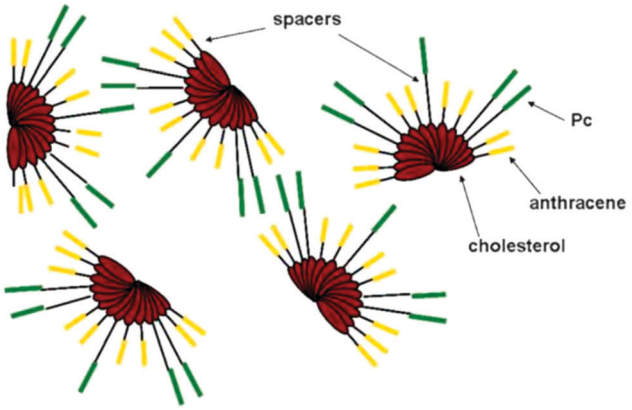

Fig. 46 The suggested self-assembly model for compounds **44–48**. Copyright 2008 Wiley. Used with permission from D. D. Díaz *et al.*, Strength Enhancement of Nanostructured Organogels through Inclusion of Phthalocyanine-Containing Complementary Organogelator Structures and *In Situ* Cross-Linking by Click Chemistry, *Chem. – Eur. J.*, Wiley.

porphyrin compounds.[49] Instead, the gels formed by compounds **45** and **46** with shorter alkyl chains were more stable upon storage compared to gels formed by compounds **47** or **48** with longer alkyl chains.[50]

Both cholesterol and Zn^{II}-Pc were observed to be necessary for the gel stabilization in the control experiments.[50] Compounds **44** and **45–48** were suggested to assemble into fan-like architectures with the cholesterol moieties at the base, enabling π-interactions between the Zn^{II}-Pc-moieties between adjacent assemblies (Fig. 46). Based on the temperature depended UV-vis- and fluorescence measurements the Zn^{II}-Pc-moieties stacked on top of each other. In addition, hydrogen bonding and van der Waals-interactions were found to promote the gel formation based on the temperature-depended FTIR-measurements. The TEM images showed the gel networks to consist of interwoven fibres. CuAAC-reaction in the gels formed by compounds **44** and **45** resulted in higher melting temperature and improved mechanical stability. Moreover, the gels were thermoreversible even after the reaction. TEM images revealed a denser and more entangled gel network after the CuAAC-reaction providing a potential explanation for the higher melting temperature. Based on the FTIR-measurements the gel structure after the reaction was stabilized by hydrogen bonding as well as by van der Waals- and π–π interactions similar to gels before the reaction.

2.6 Stimuli-responsive gels

Gels reacting specifically to either physical or chemical stimuli are defined as stimuli-responsive gels.[51] Because gels have solid- and liquid-like properties (elasticity and viscosity, respectively) and can react to stimuli in either molecular or gel network level, they are optimal materials in designing responsive materials. Physical stimuli targeting supramolecular gels include mechanical stimuli, such as shaking, as well as light and heat. Potential chemical stimuli inducing responses in supramolecular gel materials may include changes in pH or oxidation levels. If the gel contains dipoles or paramagnetic materials its properties can be affected by electric or magnetic fields. Because of the

versatility of potential sources of stimuli, physical gels can be designed to respond to more than one stimulus. This type of gels have potential for various applications in biomedicine and catalysis, for example.

Ethyl acetate gel of compound **1**, a ferrocene conjugate of cholesterol (Fig. 2), was found to react to addition of an oxidizing agent.[12] A solution of the oxidizing agent $(NH_4)_2Ce(NO_3)_6$ in methanol (1 : 1 molar ratio with respect to compound **1**) was added to the surface of the ethyl acetate gel. The yellow gel turned into a dark green suspension (Fig. 47), which was suggested to stem from the poor solubility of the oxidized form of compound **1** to methanol together with the salt effect. The repulsion between the oxidized ferrocenyl moieties was hypothesized to break the hydrogen bonds between the amide groups leading to the collapse of the gel. After the addition of a reducing agent, $SnCl_2$, the dark green suspension turned yellow indicating reduction of ferrocenyl moieties to ferrocene. However, the gel was not formed even after several heating–cooling cycles. This was most probably caused by the addition of the oxidizing agent in methanol to which compound **1** is insoluble in. Addition of NH_4NO_3 or $Ce(NO_3)_6$ did not result in similar change when added on top of the ethyl acetate gel of compound **1**.

With the help of a film mold, a cyclohexane gel of the supergelator **2** (Fig. 4) formed a gel film, which was stable in room temperature in the wet state and could be bent into a coil-like structure.[25a] The gel reacted also to four different stimuli, changing from gel to sol to gel again (Fig. 48). When a small amount of water solution containing $(NH_4)_2Ce(NO_3)_6$ (equivalent amount with respect to compound **2**) was added on top of the cyclohexane gel, it turned to dark green suspension. After adding hydrazine (1 : 1 molar ratio with respect to compound **2**) with shaking, the orange and transparent gel was re-formed. Similar to

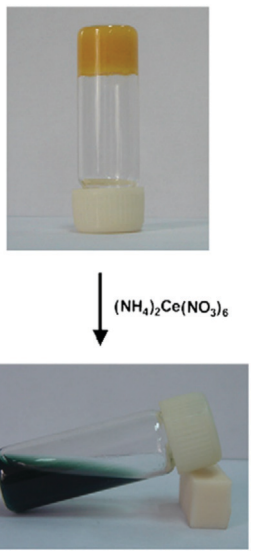

Fig. 47 Responsiveness of the ethyl acetate gel of compound **1** to an oxidizing agent. Reprinted from J. Liu *et al.*, A novel low-molecular-mass gelator with a redox active ferrocenyl group: tuning gel formation by oxidation, *J. Colloid Interface Sci.*, **318**, 397–404, Copyright 2008, with permission from Elsevier.

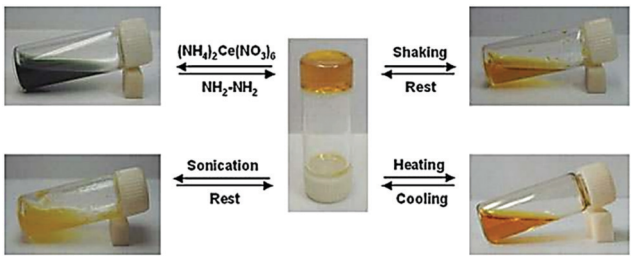

Fig. 48 Stimuli-responsiveness of the cyclohexane gel of compound **2**. Copyright 2008 Wiley. Used with permission from J. Liu *et al.*, An Organometallic Super-Gelator with Multiple-Stimulus Responsive Properties, *Adv. Mater.*, Wiley.

the ethyl acetate gel of compound **1** the simultaneous addition of NH_4NO_3 and $Ce(NO_3)_6$ did not disrupt the gel. Vigorous shaking or heating, however, resulted in solution, which restored back as gel upon resting. Sonication produced a viscous suspension, yellower in colour when compared to the original gel. When left undisturbed the suspension returned to a gel.

Also a dimeric cholesteryl ferrocene derivative (Fig. 6, compound **7**) formed a stimuli-responsive gel.[25b] In *n*-decane the thermoreversible gel reformed also after shaking and sonication at room temperature (Fig. 49). Addition of a small amount (<1/200, v/v) of capronic acid, acetic acid, or hydrochloric acid brought about the disruption of the gel. The gel did not re-form after heating and cooling without the addition of ammonia (Fig. 49). This cycle could be repeated several times, during which a precipitate (salt) formed by the acid and ammonia was observed. The collapse of the gel network was speculated to be due to the protonation of the tertiary amine leading to increased repulsion between molecules eventually resulting in the gel turning into a solution.

Interestingly, the ferrocene moiety on **7** was found to be too stable in the gel state to be oxidized by $(NH_4)Ce(NO_3)$ or $Ce(SO_4)$, for example.[25b] In dichloromethane the colour of the solution turned instantly from yellow to green upon addition of

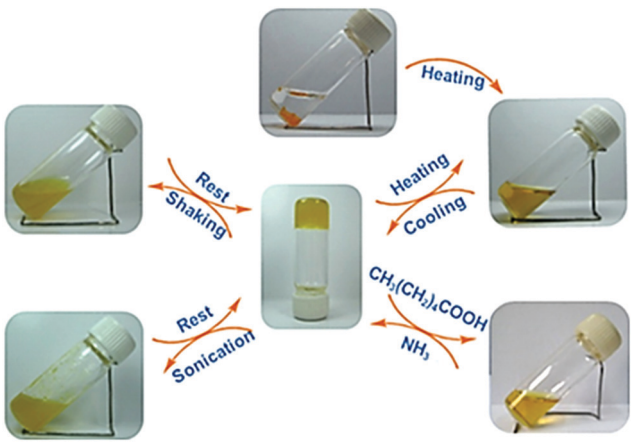

Fig. 49 Stimuli-responsiveness of the *n*-decane gel of compound **7**. Reprinted from P. He *et al.*, Preparation of novel organometallic derivatives of cholesterol and their gel-formation properties, *Colloids Surf., A*, **362**, 127–134, Copyright 2010, with permission from Elsevier.

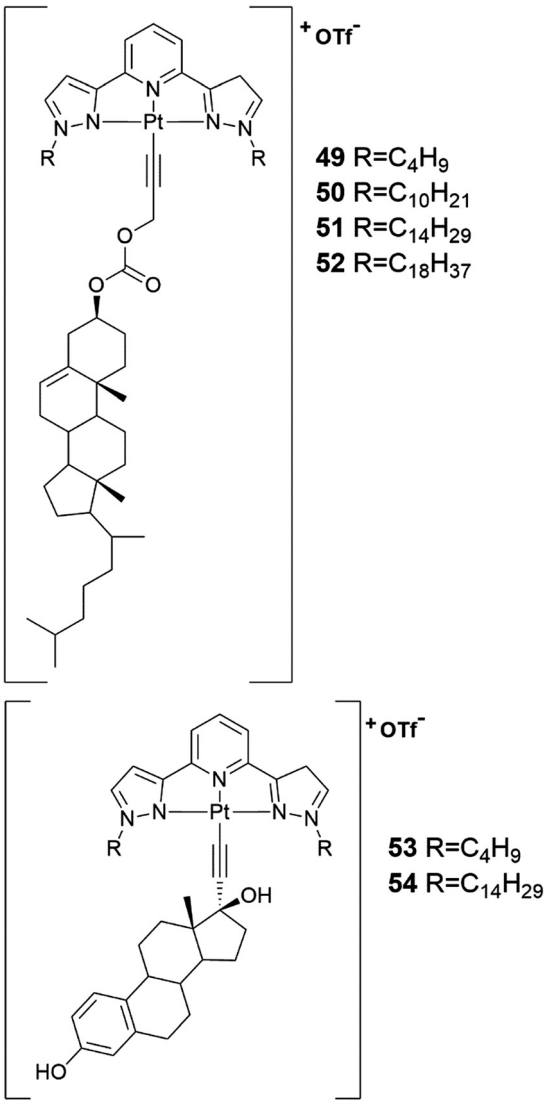

Fig. 50 The structures of the cholesterol and estradiol derivatives containing Pt-coordinating moieties **49–54**.[52]

the oxidizer, but in *n*-decane the change was much slower. Hence it was concluded that the microenvironment of the ferrocene moiety of **7** affected on the rate of the oxidation reaction.

From the cholesterol and estradiol derivatives containing Pt-coordinating moieties (Fig. 50, compounds **49–54**), three cholesterol derivatives (compounds **50–52**) formed gels in organic solvents.[52] Compound **50** formed a gel in decalin at 15 °C and compounds **51** and **52** in cyclohexane at room temperature. Compound **52** formed the most stable gel, which is why it was studied in more detail. The gel was found to re-form after heating and mechanical stress (shaking for 5 minutes).

A copper complex of compound **55** (Fig. 51) formed a gel in 1-butyronitrile (1-PrCN).[53] As the solution of Cu(I)·$\mathbf{55}_2$ complex cooled and the gel formed, an unusual distinct colour change from reddish brown to greenish blue was observed (Fig. 52). The colour change occurred repeatedly, which is why the oxidation of Cu(I) to Cu(II) was excluded. Based on the UV-vis-measurements

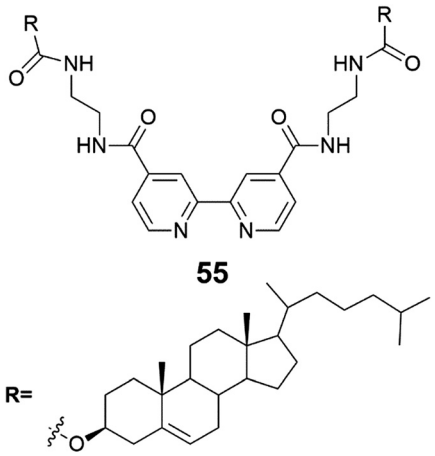

Fig. 51 Compound **55**.[53]

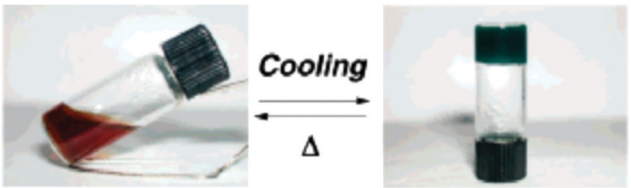

Fig. 52 Colour change of the Cu(I)·$\mathbf{55}_2$ complex as a function of the temperature in 1-PrCN. Reprinted with permission from S.-i Kawano *et al.*, *J. Am. Chem. Soc.*, 2004, **126**, 8592. Copyright 2004 American Chemical Society.

the colour change was hypothesized to originate from a distortion of the Cu(I)·$\mathbf{55}_2$ complexes to tetrahedral coordination mode caused by gel formation. The complex was confirmed to contain two molecules of compound **55** and one Cu(I) after UV-vis-measurements and gel melting temperature tests with gels containing differing amounts of Cu-ions.

The gel of Cu(I)·$\mathbf{55}_2$ in 1-PrCN turned into solution after adding ascorbic acid and heating following by the re-formation of a greenish blue gel during cooling.[53] Addition of $NOBF_4$ with heating resulted in a solution with a small amount of pale-blue precipitate (Fig. 53), which after adding ascorbic acid with heating formed the gel again. Based on the UV-vis-, CD-, and TEM-measurements the properties of the gel that re-formed after addition of the oxidizing agent were similar to the original gel formed by the Cu(I)·$\mathbf{55}_2$ complex in 1-PrCN.

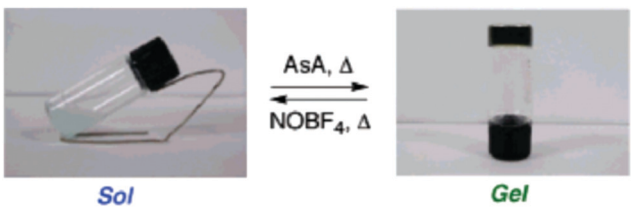

Fig. 53 Cu(I)·$\mathbf{55}_2$ gel in 1-PrCN responding to oxidizing and reducing agents. Reprinted with permission from S.-i Kawano *et al.*, *J. Am. Chem. Soc.*, 2004, **126**, 8592. Copyright 2004 American Chemical Society.

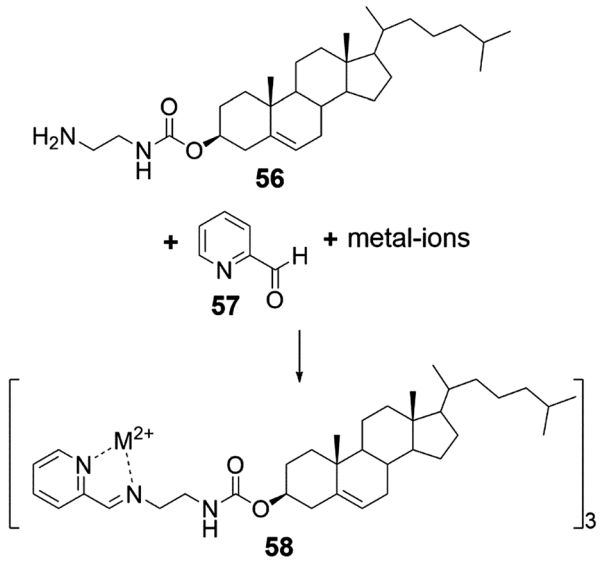

Fig. 54 *In situ* preparation of the gelator **58** by subcomponent self-assembly.[48]

A cholesteryl amide derivative **56** was used in producing metallogels responding to multiple stimuli by subcomponent self-assembly method (Fig. 54 and 55).[48] When mixing the components forming the eventual gelator *in situ* in 3 : 3 : 1 ratio (**56** : **57** : metal ion, respectively) at room temperature a gel was formed. The mixing order was irrelevant. The metal-complexation could be seen with naked eye being colourless to green in the case of Cu(II), to yellow in the case of Ni(II), and to pale-yellow in the case of Zn(II). Gels formed also with a mixture of metal ions, provided that the overall ligand : metal ion ratio was 3 : 1. This opens up possibilities to fine-tune the properties of the metallogel. The gels were mainly formed in alcohols, although partial gels were formed in certain other organic solvents by Ni(II)- and Zn(II)-complexes as well. The gels were transparent in 1-heptanol and 1-octanol in the case of Cu(II)- and Zn(II)-complexes, but opaque in 1-pentanol and 1-hexanol. The gels formed by the Ni(II)-complex were transparent.

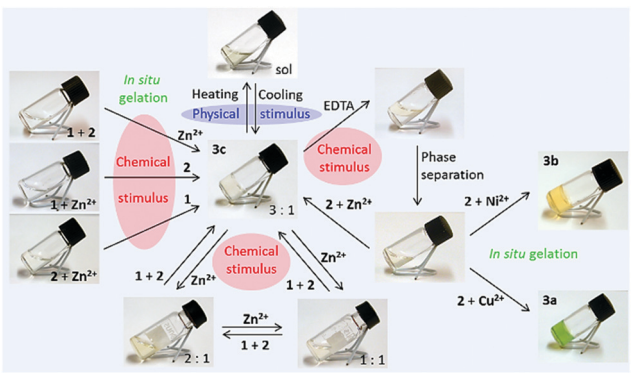

Fig. 55 Response to multiple stimuli by gel of Zn(II)-complex of **58** as 1% (w/v) in 1-octanol. Copyright 2013 Wiley. Used with permission from H. Bunzen *et al.*, Subcomponent Self-Assembly: A Quick Way to New Metallogels, *Chem. – Eur. J.*, Wiley.

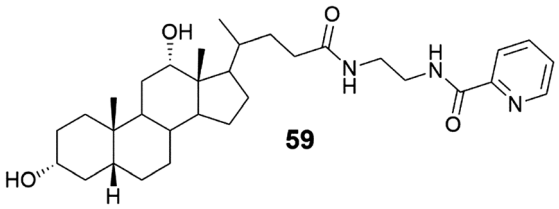

Fig. 56 The structure of the deoxycholic acid derivative **59** capable of forming Cu(II)-metallogels.[54]

The thermal stability and strength of the gels was observed to be better in higher alcohols.[48] Gels formed by Ni(II)-complex were thermally the most stable with melting temperatures of the 2% gel (w/v) in higher alcohols being $>95\ ^{\circ}C$. Moreover, the Ni(II)-complex acted as a supergelator in 1-octanol, forming a gel even as low a concentration as 0.07% (w/v). The complex **58** formed thermoreversible gels in 1-octanol with each metal ion used in the study (Fig. 55, Zn(II)-complex as an example). Excess of metal-salt resulted in a collapse of the gel. Based on MS-measurements, 2 : 1 and 1 : 1 ligand : metal complexes did not form the gels, whereas the 3 : 1 complex acted as a gelator. After addition of a strong chelating agent (EDTA) the gel turned into a solution. After phase separation the gel could be recovered by adding metal salt, the same or different than the original one, or a mixture of metal salts providing a possibility to change the properties of the gels in a relatively simple manner when needed.

Deoxycholic acid derivative (Fig. 56, compound **59**) was found to self-assemble into a gel only in the presence of copper salt.[54] The copper salt solution was added to the aqueous solution of **59** containing methanol, acetone, or acetonitrile (30–50%). The molar ratios of **59** : salt were 2 : 1, 1 : 1, and 1 : 2, respectively. The effect of the counter ion was studied by utilizing three different salts in the gelation tests. In the case of $CuCl_2{\cdot}2H_2O$ only transparent blue solutions were formed. When using $CuSO_4{\cdot}5H_2O$ gels were formed in all ratios, predominantly during the ultrasound treatment before heating. These gels were not as stable as the gels formed with copper nitrate ($Cu(NO_3)_2{\cdot}3H_2O$), with which gels were formed during ultrasound treatment in ratios of 1 : 1 and 1 : 2. Some of the systems studied formed a gel even the day after the heating when shaking the sample vigorously. Based on the NMR-measurements with different **59** : Cu(II) ratios, the pyridine moiety was found to be a prerequisite for the gel formation, although the gel was formed by complexes having various **59** : Cu(II) ratios revealed by MS-measurements performed for the dissolved gel samples.

The Cu(II)-metallogels formed by **59** collapsed as a result of adding a few drops of pyridine, triethyl amine, aquoeus ammonia, or a small amount of disodium salt of **EDTA** (Fig. 57).[54] Redox-responsiveness of the gels was also observed (Fig. 58). Water solution of ascorbic acid afforded in reduction of the Cu(II)-ions to Cu(I)-ions indicated by the colour change of the sample. During cooling the solution turned from transparent to opaque, and after shaking the sample changed colour to green with some green precipitate. Addition of 0.5 M nitric acid with heating and ultrasound treatment re-formed the gel as a result of oxidation of the copper ions.

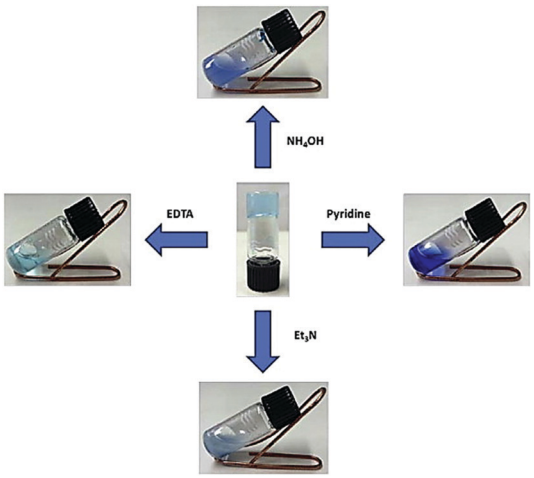

Fig. 57 The response of Cu(II)-metallogels of **59** to chemical stimuli. Reprinted from V. Noponen *et al.*, Stimuli-responsive bile acid-based metallogels forming in aqueous media, *Steroids*, **97**, 54–61, Copyright 2015, with permission from Elsevier.

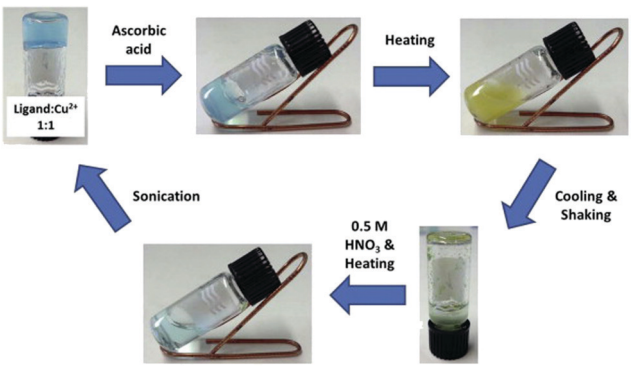

Fig. 58 Redox-response of Cu(II)-metallogels of **59**. Reprinted from V. Noponen *et al.*, Stimuli-responsive bile acid-based metallogels forming in aqueous media, *Steroids*, **97**, 54–61, Copyright 2015, with permission from Elsevier.

3 Summary and outlook

Gels are part of our everyday lives in the fields of for example cosmetics, pharmaceutics, food industry, catalysis, and coatings. Differing from the traditional polymeric gels, supramolecular gels are formed by self-assembly driven by weak interactions, such as hydrogen bonding or electrostatic, van der Waals, hydrophobic, or π–π interactions. With their reversibility and versatility supramolecular gels can be designed to respond to chemical and physical stimuli. Metal–ligand coordination may lead to metallogels possessing multi-responsive properties to wide environmental responses. Electro- or magneto-responsive metallogels have potential when designing valves, clutches, or dampers, whereas metallogels containing lanthanoids or transition metals show thermo-, mechano-, chemo-, and photo-responsiveness.[55,56]

Particularly from the biomedical and pharmacological point of views, steroid-derived supramolecular gels with their biocompatible nature are auspicious. Steroidal metallogels may find lifesaving applications in the detection of disease markers or specific drugs. Furthermore, they may be utilized in site-specific and controlled drug delivery, cell separation, immunoassay, magnetic resonance imaging, gene delivery, minimally invasive surgery, radionuclide therapy, hyperthermia, or even artificial muscle applications.

Due to the rigid and chiral steroidal skeleton accommodating different derivatizable functional groups steroids and their derivatives have tremendous potential in forming gels with variable properties and applications. Even minuscule changes in the structure of the gelator may change not only the gelation tendencies but also the characteristics of the gels significantly. As a result, the spectrum of potential materials is extremely rich with countless potential applications waiting to be charted.

Conflicts of interest

There are no conflicts to declare.

Acknowledgements

The authors are grateful to Ms Saana Rekola for updating the list of references and for Dr Hana Bunzen for the colour version of Fig. 54. University of Jyväskylä is acknowledged for financial support.

References

1 (*a*) S. B. Schryver, *Proc. R. Soc. London, Ser. B*, 1913, **86**, 460; (*b*) S. B. Schryver, *Proc. R. Soc. London, Ser. B*, 1914, **87**, 366; (*c*) S. B. Schryver, *Proc. R. Soc. London, Ser. B*, 1916, **89**, 176; (*d*) S. B. Schryver, *Proc. R. Soc. London, Ser. B*, 1916, **89**, 361.
2 P. M. Dewick, *Medicinal Natural Products: a Biosynthetic Approach*, Wiley, Great-Britain, 2009, ch. 5, pp. 247–298.
3 V. Piironen, D. G. Lindsay, T. A. Miettinen, J. Toivo and A.-M. Lampi, *J. Sci. Food Agric.*, 2000, **80**, 939.
4 (*a*) J. W. Steed and J. L. Atwood, *Supramol. Chem.*, Wiley, Great-Britain, 2009, ch. 14, pp. 888–893; (*b*) J. W. Steed, *Chem. Commun.*, 2011, **47**, 1379.
5 (*a*) K. Rajangam, H. A. Behanna, M. J. Hui, X. Han, J. F. Hulvat, J. W. Lomasney and S. I. Stupp, *Nano Lett.*, 2006, **6**, 2086; (*b*) V. Jayavarna, M. Ali, T. A. Jowitt, A. F. Miller, A. Saiani, J. E. Gough and R. V. Ulijn, *Adv. Mater.*, 2006, **18**, 611.
6 A. R. Hirst, B. Escuder, J. F. Miravet and D. K. Smith, *Angew. Chem., Int. Ed.*, 2008, **47**, 8002.
7 L. Mao, H. Wang, M. Tan, L. Ou, D. Kong and Z. Yang, *Chem. Commun.*, 2012, **48**, 395.
8 A. Feinle, M. S. Elsaesser and N. Hüsing, *Chem. Soc. Rev.*, 2016, **45**, 3377.
9 (*a*) K. Ghosh and D. Kar, *Org. Biomol. Chem.*, 2012, **10**, 8800; (*b*) K. Ghosh, D. Kar and S. Bhattacharya, *Supramol. Chem.*, 2014, **26**, 313; (*c*) K. Ghosh, D. Kar, S. Panja and S. Bhattacharya, *RSC Adv.*, 2014, **4**, 3798; (*d*) K. Ghosh and S. Panja, *RSC Adv.*, 2015, **5**, 12094; (*e*) K. Ghosh, A. Panja and S. Panja, *New J. Chem.*, 2016, **40**, 3476; (*f*) K. Ghosh and S. Panja,

ChemistrySelect, 2016, **1**, 3667; (*g*) Y. Wang, Z. Wang, Z. Xu, X. Yu, K. Zhao, Y. Li and X. Pang, *Org. Biomol. Chem.*, 2016, **14**, 2218; (*h*) K. Ghosh and S. Panja, *Supramol. Chem.*, 2017, **29**(5), 350; (*i*) K. Ghosh, S. Panja and S. Bhattacharya, *ChemistrySelect*, 2017, **2**, 959; (*j*) S. Panja, S. Bhattacharya and K. Ghosh, *Langmuir*, 2017, **33**, 8277.

10 M. O.-M. Piepenbrock, G. O. Lloyd, N. Clarke and J. W. Steed, *Chem. Rev.*, 2010, **110**, 1960.

11 Y. Qiao, Y. Lin, Z. Yang, H. Chen, S. Zhang, Y. Yan and J. Huang, *J. Phys. Chem. B*, 2010, **114**, 11725.

12 J. Liu, J. Yan, X. Yuan, K. Liu, J. Peng and Y. Fang, *J. Colloid Interface Sci.*, 2008, **318**, 397.

13 (*a*) J. Zhang and C. Y. Su, *Coord. Chem. Rev.*, 2010, **110**, 1373; (*b*) F. Fages, *Angew. Chem., Int. Ed.*, 2008, **45**, 1680; (*c*) T. Gorai and U. Maitra, *Angew. Chem., Int. Ed.*, 2017, **56**, 10730.

14 A. Y.-Y. Tam and V. W.-W. Yam, *Chem. Soc. Rev.*, 2013, **42**, 1540.

15 For example: (*a*) S. Bhowmik, S. Banerjee and U. Maitra, *Chem. Commun.*, 2010, **46**, 8642; (*b*) S. Banerjee, R. Kandanelli, S. Bhowmik and U. Maitra, *Soft Matter*, 2011, **7**, 8207; (*c*) R. Kandanelli, A. Sarkar and U. Maitra, *Dalton Trans.*, 2013, **42**, 15381; (*d*) R. Laishram and U. Maitra, *ChemistrySelect*, 2018, **3**, 519.

16 For example: (*a*) H. Wang, S. Song, J. Hao and A. Song, *Chem. – Eur. J.*, 2015, **21**, 12194; (*b*) H. Wang, W. Xu, S. Song, L. Feng, A. Song and J. Hao, *J. Phys. Chem. B*, 2014, **118**, 4693; (*c*) Y. Qiao, H. Chen, Y. Lin, Z. Yang, X. Cheng and J. Huang, *J. Phys. Chem. C*, 2011, **115**, 7323; (*d*) Y. Qiao, Y. Wang, Z. Yang, Y. Lin and J. Huang, *Chem. Mater.*, 2011, **23**, 1182.

17 A. Chakrabarty, U. Maitra and A. D. Das, *J. Mater. Chem.*, 2012, **22**, 18268.

18 M. Maity and U. Maitra, *J. Mater. Chem. A*, 2014, **2**, 18952.

19 S. Bhowmik, T. Gorai and U. Maitra, *J. Mater. Chem. C*, 2014, **2**, 1597.

20 (*a*) R. Laishram and U. Maitra, *Asian J. Org. Chem.*, 2017, **6**, 1235; (*b*) T. Gorai and U. Maitra, *J. Mater. Chem. B*, 2018, **6**, 2143; (*c*) S. Bhowmik and U. Maitra, *Chem. Commun.*, 2012, **48**, 4624.

21 H. Wang, W. Xu, S. Song, L. Feng, A. Song and J. Hao, *J. Phys. Chem. B*, 2015, **118**, 4639.

22 R. Laishram, S. Bhowmik and U. Maitra, *J. Mater. Chem. C*, 2015, **3**, 5885.

23 (*a*) J. C. Medina, I. Gay, Z. Chen, L. Echegoyen and G. W. Gokel, *J. Am. Chem. Soc.*, 1991, **113**, 365; (*b*) K. Wang, S. Muños, L. Zhang, R. Castro, A. E. Kaifer and G. W. Gokel, *J. Am. Chem. Soc.*, 1996, **118**, 6707.

24 T. Klawonn, A. Gansäuer, I. Winkler, T. Lauterbach, D. Franke, R. J. M. Nolte, M. C. Feiters, H. Börner, J. Hentschel and K. H. Dötz, *Chem. Commun.*, 2007, 1894.

25 (*a*) J. Liu, P. He, J. Yan, X. Fang, J. Peng, K. Liu and Y. Fang, *Adv. Mater.*, 2008, **20**, 2508; (*b*) P. He, J. Liu, K. Liu, L. Ding, J. Yan, D. Gao and Y. Fang, *Colloids Surf., A*, 2010, **362**, 127; (*c*) J. Yan, J. Liu, Y. Sun, P. Jing, P. He, D. Gao and Y. Fang, *J. Phys. Chem. B*, 2010, **114**, 13116.

26 C. E. Housecroft and A. G. Sharpe, *Inorganic Chemistry*, Pearson Education Limited, England, 2008, ch. 24, pp. 841–845.

27 A. Gansäuer, I. Winkler., T. Klawonn, R. J. M. Nolte, M. C. Feiters, H. G. Börner, J. Hentschel and K. H. Dötz, *Organometallics*, 2009, **28**, 1377.

28 (*a*) V. S. Sajisha and U. Maitra, *Chimia*, 2013, **67**, 44; (*b*) Y. Okamoto and J. Kido, *Chem. Rev.*, 2002, **102**, 2357.

29 (*a*) M. Maity and U. Maitra, *Dalton Trans.*, 2017, **46**, 9266; (*b*) Y. Qiao, Y. Lin, Y. Wang, Z. Yang, J. Liu, J. Zhou, Y. Yan and J. Huang, *Nano Lett.*, 2009, **9**(12), 4500.

30 (*a*) S. Chatterjee and U. Maitra, *Nanoscale*, 2016, **8**, 14979; (*b*) S. Chatterjee and U. Maitra, *Nanoscale*, 2017, **9**, 13820.

31 T. Gorai and U. Maitra, *ACS Sens.*, 2016, **1**, 934.

32 Y. Qiao, Y. Lin, S. Zhang and J. Huang, *Chem. – Eur. J.*, 2011, **17**, 5180.

33 Y. Wang, X. Xin, W. Li, C. Jia, L. Wang, J. Shen and G. Xu, *J. Colloid Interface Sci.*, 2014, **431**, 82.

34 R. Laishram and U. Maitra, *Chem. – Asian J.*, 2017, **12**, 1267.

35 (*a*) N. M. Sangeetha, R. Balasubramanian, U. Maitra, S. Ghosh and A. R. Raju, *Langmuir*, 2002, **18**, 7154; (*b*) N. M. Sangeetha, S. Bhat, A. Choudhury, U. Maitra and P. Terech, *J. Phys. Chem. B*, 2004, **108**, 16056; (*c*) S. Bhat and U. Maitra, *Tetrahedron*, 2007, **63**, 7309.

36 For example: (*a*) V. Noponen, Nonappa, M. Lahtinen, A. Valkonen, H. Salo, E. Kolehmainen and E. Sievänen, *Soft Matter*, 2010, **6**, 3789; (*b*) M. Löfman, J. Koivukorpi, V. Noponen, H. Salo and E. Sievänen, *J. Colloid Interface Sci.*, 2011, **360**, 633; (*c*) V. Noponen, H. Belt, M. Lahtinen, A. Valkonen, H. Salo, J. Ulrichová, A. Galandáková and E. Sievänen, *Steroids*, 2012, **77**, 193; (*d*) V. Noponen, A. Valkonen, M. Lahtinen, H. Salo and E. Sievänen, *Supramol. Chem.*, 2013, **25**, 133; (*e*) R. Kuosmanen, R. Puttreddy, R.-M. Willman, I. Äijäläinen, A. Galandáková, J. Ulrichová, H. Salo, K. Rissanen and E. Sievänen, *Steroids*, 2016, **108**, 7.

37 J.-S. Shen, Y.-L. Chen, J.-L. Huang, J.-D. Chen, C. Zhao, Y.-Q. Zheng, T. Yu, Y. Yang and H.-W. Zhang, *Soft Matter*, 2013, **9**, 2017.

38 B. Kuppan and U. Maitra, *ChemNanoMat*, 2018, **4**, 846.

39 T. Tu, W. Fang, X. Bao, X. Li and K. H. Dötz, *Angew. Chem., Int. Ed.*, 2011, **50**, 6601.

40 Y. Li, A. Y.-Y. Tam, K. M.-C. Wong, W. Li, L. Wu and V. W.-W. Yam, *Chem. – Eur. J.*, 2011, **17**, 8048.

41 K. Liu, L. Meng, S. Mo, M. Zhang, Y. Mao, X. Cao, C. Huang and T. Yi, *J. Mater. Chem. C*, 2013, **1**, 1753.

42 M. Dukh, D. Šaman, J. Kroulik, I. Černý, V. Pouzar, V. Král and P. Drašar, *Tetrahedron*, 2003, **59**, 4069.

43 S. Malik, S.-I. Kawano, N. Fujita and S. Shinkai, *Tetrahedron*, 2007, **63**, 7326.

44 A. Panja and K. Ghosh, *Mater. Chem. Front.*, 2018, **2**, 2286.

45 G. Liu, J. Sheng, W. L. Teo, G. Yang, H. Wu, Y. Li and Y. Zhao, *J. Am. Chem. Soc.*, 2018, **140**, 16275.

46 S. Debnath, J.-F. Bergamini, F. Artzner, C. Mériadec, F. Camerel and M. Fourmigué, *Chem. Commun.*, 2012, **48**, 2283.

47 K. Murata, M. Aoki, T. Nishi, A. Ikeda and S. Shinkai, *J. Chem. Soc., Chem. Commun.*, 1991, **0**, 1715.

48 H. Bunzen, Nonappa, E. Kalenius, S. Hietala and E. Kolehmainen, *Chem. – Eur. J.*, 2013, **19**, 12978.

49 T. Ishi-i, R. Iguchi, E. Snip, M. Ikeda and S. Shinkai, *Langmuir*, 2001, **17**, 5825.

50 D. D. Díaz, J. J. Cid, P. Vázquez and T. Torres, *Chem. – Eur. J.*, 2008, **14**, 9261.
51 P. Terech and R. G. Weiss, *Molecular Gels – Materials with Self-Assembled Fibrillar Networks*, Springer, Netherlands, 2006, ch. 27, pp. 895–927.
52 Y. Li, E. S.-H. Lam, A. Y.-Y. Tam, K. M. C. Wong, W. H. Lam, L. Wu and V. W.-W. Yam, *Chem. – Eur. J.*, 2013, **19**, 9987.
53 S.-i. Kawano, N. Fujita and S. Shinkai, *J. Am. Chem. Soc.*, 2004, **126**, 8592.
54 V. Noponen, K. Toikkanen, E. Kalenius, R. Kuosmanen, H. Salo and E. Sievänen, *Steroids*, 2015, **97**, 54.
55 B. Xing, M. Choi and B. Xu, *Chem. – Eur. J.*, 2002, **8**, 5028.
56 W. Weng, J. Beck, A. Jamieson and S. Rowan, *J. Am. Chem. Soc.*, 2006, **128**, 11663.

